TRANSVERSERLY ISOTROPIC SATURATED POROUS FORMATIONS: I. THEORETICAL DEVELOPMENTS AND (QUASI) BODY WAVE PROPERTIES

by

D.P. Schmitt*

Earth Resources Laboratory
Department of Earth, Atmospheric, and Planetary Sciences
Massachusetts Institute of Technology
Cambridge, MA 02139

ABSTRACT

Using the results of homogenization theory, the constitutive equations for an anisotropic porous formation saturated by a Newtonian viscous fluid are derived. The transverse isotropy situation is investigated in terms of partial stresses in both phases. It allows to take into account a transversely isotropic skeleton and/or a transversely isotropic complex permeability tensor whose axes of symmetry are assumed to coincide. The wavenumbers equations are solved as part of a cylindrical geometry and general solutions for the displacement potentials in each phase are presented.

Four dispersive and dissipative waves propagate in a transversely isotropic saturated porous formation: two quasi compressional waves, a quasi SV wave and a SH wave. All three quasi body waves approach the isotropic P_1 wave, slow P_2 wave, and S wave only as the degree of anisotropy of both the skeleton and the complex permeability tensor vanishes. Simple analytical formuale are derived for vertical and horizontal propagations. The SH-wave only excites the horizontal permeability, whatever its angle of propagation with respect to the vertical. The velocities and attenuations of these four waves are studied as a function of the only transversely isotropic permeability, the anisotropy of the skeleton, and the anisotropy of the mass coupling coefficient.

Whatever the frequency, the quasi P_1-wave, quasi SV-wave and SH-wave velocities are primarily governed by the anisotropy of the skeleton. Contrary, the quasi slow P_2-wave velocity is mostly representative of the complex permeability tensor transverse isotropy. At very high frequencies, when the inertial forces in the saturated porous formation are dominant, an anisotropy of the mass coupling coefficient leads to slightly

*Now at Etudes et Productions Schlumberger, 26 Rue de la Cavée, 92142 Clamart, France.

different quasi SV-wave velocities along the principal directions, contrary to the pure elastic situation. For the quasi P_1 wave and the quasi SV wave, the degree of anisotropy of the strongly frequency dependent attenuation induced by the two phase character of the material is more important than that of the velocity.

INTRODUCTION

Reservoirs are known to be anisotropic. Such biphase media can be modeled by a solid anisotropic elastic skeleton permeated by an anisotropic network of interconnected pores saturated by a compressible viscous liquid. The general constitutive equations for an anisotropic saturated porous formation with uniform (i.e., equant) porosity have been first described by Biot (1955). Two main other papers by the same author (Biot, 1962a, b)"describe" the phenomena in terms of total stress, relative fluid displacement and non uniform porosity. In this paper, homogenization theory (Auriault, 1980, 1983, 1986; Auriault et al., 1985) is followed. It allows a comprehensive and unified definition of frequency dependent viscous and mass coupling coefficients. The constitutive equations for a general anisotropic saturated porous formation are first presented along with the physical asssumptions. Both total stress and partial stresses formulations are given. The equations for the transversely isotropic case are then derived as part of the latter formulation with a comprehensive discussion of the different needed parameters. The equations relative to the isotropic situtation and to an elastic formation are then deduced.

Few authors investigated wave propagation in transversely isotropic saturated porous formations. Badiey and Yamamoto (1985) considered plane wave propagation in the sea floor. Neglecting the slow P_2 wave, they somehow mixed the equations of motion relative to a transversely isotropic elastic formation with the formulae of the velocities for the fast P_1 and S waves in an isotropic saturated porous formation. Yew and Weng (1987) studied the reflection of plane waves at a water-transversely isotropic saturated porous ice interface. They used Biot (1962a) formualtion, evaluating the elastic coefficients with a composite material model. In the second section, we derived the wavenumbers equations as part of a cylindrical geometry used in full waveform logging. General solutions for the displacement potentials in each phases are presented. The case of the only transversely isotropic permeability is discussed, followed by the complete isotropic saturated porous situation and the elastic case. The last section is devoted to an analytical and numerical study of the (quasi) body wave phase velocities and attenuations.

CONSTITUTIVE EQUATIONS

Anisotropic Saturated Porous Formation

A detailed discussion of the homogenization process is out of the scoop of this paper. As a reminder, following Boutin (1987), let us say that it uses two scales; the microscopic and the macroscopic ones. Their characteristic lengths, i.e., that of the grains (l) and of the studied volume (L), are defined so that

$$\frac{l}{L} = \epsilon << 1 \,. \tag{1}$$

The description of a physical phenomenon governed by a function $\mathcal{F}$ requires the definition of two interdependent spatial variables coordinates systems, X and y. X refers to the macroscopic scale, for which $L = 0(1)$ and $l = 0(\epsilon)$; while y is associated with the microscopic scale for which $l = 0(1)$ and $L = 0(1/\epsilon)$. The interdependence is, of course,

$$X = \epsilon y \,. \tag{2}$$

y describes the fast variations about a mean value, while X describes the slow variations. Therefore, the function $\mathcal{F}$ is defined as

$$\mathcal{F} = \mathcal{F}(X, y) = \mathcal{F}(X, X/\epsilon) \,. \tag{3}$$

Only the smooth variations defined by X are reachable at the macroscopic scale. Knowing the equations satisfied by $\mathcal{F}(X, X/\epsilon)$ which govern the phenomena at the microscopic scale, the homogenization process looks for the equations satisified by a function $F(X)$ defined as

$$F(X) = \lim_{\epsilon \to 0} \mathcal{F}(X, X/\epsilon) \,. \tag{4}$$

Taking the limit is equivalent to reduce the size of the heterogeneities to zero: the medium is homogenized. For practical purpose, $\epsilon << 1$ is sufficient.

Assumptions

The description of a continuum equivalent to a saturated porous material is based on the following assumptions: (1) the fine structure (i.e., at the microscopic scale) is spatially periodic, (2) the study is made as part of the linear theory of elasticity, (3) the material is fully saturated by a compressible viscous Newtonian fluid, (4) the stresses and the densities of the skeleton and the saturant fluid are of the same

order of magnitude, (5) the system is at equilibrium when at rest, (6) the process is purely mechanical (no thermo-mechanical coupling, for example, is considered), (7) the wavelength is supposed to be large compared to the characteristic pore dimension (i.e., no diffraction), (8) the fluid flow is linear (i.e., the convection terms are negligible with respect to the viscous terms), (9) the viscous and inertial terms are of the same order of magnitude and, (10) the porosity is uniform. Despite many controversial discussions, this assumption is not so restrictive. Moreover, practical calculations are most of the time performed as part of it.

The derivation is based on the very strong asspumption (1) of microscopic spatial periodicity. The function $\mathcal{F}(X, y)$ is thus defined as an asymptotic series of powers of ϵ, i.e.,

$$\mathcal{F}(X, y) = \sum_{i=0}^{\infty} \epsilon^i \mathcal{F}^{(i)}(X, X/\epsilon) \,, \tag{5}$$

where each funtion $\mathcal{F}^{(i)}$ is periodic with y, the period being identical.

The solution is obtained by identifying term by term the coefficients of the powers of ϵ in the microscopic equations written with asymptotic series. Theoretically, one specific system should be solved for each $\mathcal{F}^{(i)}$ before checking the convergence of the series. When ϵ is small enough (i.e., $\epsilon \leq 10^{-2}$), the very first term is sufficient to describe the equivalent medium. Checking the physical meaning of the obtained variables is the final step (Auriault, 1980; 1983, Boutin, 1987). Besides the periodicity criterion, the two most important assumptions are (2) and (8) as they ensure the unicity of the solution.

Without loosing any fundamental generality, one additional (quite usual) assumption is made in the present paper: (11) the constitutive grains are homogeneous and isotropic. Finally, from the anisotropy point of view, two last assumptions are stated which allow "easy" analytical developments: (12) the principal directions of the skeleton coincide with those of the reference axes and, (13) the permeability tensor and the skeleton have the same principal directions.

Total Stress Formulation

Using the first nine assumptions listed above, the homogenization process leads to the following constitutive equations (Auriault, 1980, 1986):

$$\text{Macroscopic behavior law :} \quad \underline{\underline{\Sigma}} = \underline{\underline{c}} \cdot \underline{\underline{e}} - \underline{\underline{\alpha}}\, p \,, \tag{6}$$

$$\text{Dynamics equation :} \quad \nabla \cdot \underline{\underline{\Sigma}} = \overline{\rho_s}\, \underline{\ddot{u}} + \tilde{\varphi} \rho_f \underline{\ddot{U}} \,, \tag{7}$$

$$\text{Generalized Darcy's law}: \quad \tilde{\varphi}\left(\dot{\underline{U}} - \dot{\underline{u}}\right) = \underline{\underline{K}}(\omega)\left\{-\rho_f \ddot{\underline{u}} - \nabla p\right\} , \tag{8}$$

$$\text{Balance of macroscopic volume}: \quad \nabla \cdot \tilde{\varphi}\,(\underline{U} - \underline{u}) = -\underline{\underline{\alpha}} \cdot \underline{\underline{e}} - \beta p . \tag{9}$$

In the above equations, $\underline{\underline{\Sigma}}$ is the total stress tensor (i.e., $\underline{\underline{\Sigma}} \cdot \underline{n} ds$ is the force acting on a facet of the homogenized medium whose surface is ds and normal is $\underline{n}$); $\underline{\underline{c}}$ is the stiffnes tensor of the skeleton at the macroscopic scale; $\underline{\underline{e}}$ is the strain tensor of the skeleton at the macroscopic scale; and p is the saturant fluid pressure. $\underline{u} = (u,\ v,\ w)^T$ and $\underline{U} = (U,\ V,\ W)^T$ are, respectively, the solid and saturant fluid displacement vectors at the macroscopic scale. $\tilde{\varphi}$ is the porosity of the material, i.e., the fluid volume $|\Omega_f|$ to the total volume $|\Omega|$ ratio. $\overline{\rho_s} = \dfrac{1}{|\Omega|}\displaystyle\int_\Omega \rho_s \, d\Omega$ represents the skeleton density while ρ_s is the constitutive grains density. ρ_f is the saturant fluid density. $\underline{\underline{\alpha}}$ is an elastic tensor, and β is a compressibility coefficient. Finally, ω is the angular frequency, while $\underline{\underline{K}}(\omega)$ is the complex permeability tensor. The generalized Darcy's law is a hereditary dynamic equation (i.e., memory effect). In the time domain, the second member becomes a convolution equation. Hence, the knowledge of the filtration velocity at a given time requires that of $\nabla p_t + \rho_f \ddot{\underline{u}}_t$ any time before.

Denoting $\underline{\underline{\Delta}}$ the compliance tensor of the constitutive grains,

$$\alpha_{kl} = \delta_{kl} - c_{mnkl}\,\Delta_{mntt} , \tag{10}$$

and

$$\beta = (1 - \tilde{\varphi})\Delta_{iill} - c_{kkij}\Delta_{khtt}\Delta_{ijll} + \frac{\tilde{\varphi}}{K_f} , \tag{11}$$

where δ_{kl} is the Kronecker symbol and the Einstein convention is used. K_f is the saturant fluid bulk modulus.

Because of assumptions (10) and (11), denoting λ_1 and μ_1 the Lamé coefficients of the constitutive grains and $K_s = \lambda_1 + \dfrac{2}{3}\mu_1$ the corresponding bulk modulus, one has:

$$\overline{\rho_s} = (1 - \tilde{\varphi})\rho_s , \tag{12}$$

$$\Delta_{khtt} = \frac{\delta_{kh}}{3K_s} , \ \text{so that} \ \ \Delta_{kktt} = \frac{1}{K_s} . \tag{13}$$

Equations (10) and (11) then become:

$$\alpha_{kl} = \delta_{kl} - c_{ppkl}\frac{1}{3K_s} , \tag{14}$$

$$\beta = -\frac{1}{9K_s^2}c_{kkhh} + \frac{(1 - \tilde{\varphi})}{K_s} + \frac{\tilde{\varphi}}{K_f} . \tag{15}$$

Such formulae imply that the coefficients are independent from the pore fluid pressure. Brown and Korringa (1975) discussed this dependence for a complete isotropic material.

The complex (dynamic) permeability tensor is always positive, definite, symmetric and thus invertible (Auriault, 1980, 1986; Auriault et al., 1985). Boutin (1987) has also shown that its real and imaginary parts, respectively $\underline{\underline{K_R}}(\omega)$ and $\underline{\underline{K_I}}(\omega)$, verify the Kramers-Koening theorem, i.e., are Hilbert transform of one another:

$$\underline{\underline{K_R}}(\omega) = \frac{1}{\pi} P.V. \int_{-\infty}^{+\infty} \frac{\underline{\underline{K_I}}(X)}{\omega - X} dX , \tag{16}$$

$$\underline{\underline{K_I}}(\omega) = \frac{1}{\pi} P.V. \int_{-\infty}^{+\infty} \frac{\underline{\underline{K_R}}(X)}{\omega - X} dX , \tag{17}$$

where *P.V.* stands for Cauchy's principal value. In the time domain the causal permeability tensor $\underline{\underline{K}}(t)$ is real. $\underline{\underline{K_R}}(\omega)$ is then even and $\underline{\underline{K_I}}(\omega)$ is odd, so that the above relations can be written as

$$\underline{\underline{K_R}}(\omega) = \frac{1}{\pi} P.V. \int_{0}^{+\infty} \frac{\underline{\underline{K_I}}(X)}{\omega^2 - X^2} dX , \tag{18}$$

$$\underline{\underline{K_I}}(\omega) = \frac{1}{\pi} P.V. \int_{0}^{+\infty} \frac{\underline{\underline{K_R}}(X)}{\omega^2 - X^2} dX . \tag{19}$$

These relations emphasize the interdependence of $\underline{\underline{K_R}}(\omega)$ and $\underline{\underline{K_I}}(\omega)$ but are of few practical interest as they require the knowledge of one of them in the entire frequency range. They also show that if the principal directions of $\underline{\underline{K_R}}(X)$ are frequency independent, then $\int_{-\infty}^{+\infty} \frac{\underline{\underline{K_R}}(X)}{\omega - X} dX$, and then $\underline{\underline{K_I}}(X)$, are diagonal in the same axes, i.e., have the same principal directions (and reciprocally).

The tensor which is in fact used is the inverse, $\underline{\underline{H}}(\omega) = \underline{\underline{K}}^{-1}(\omega) = \underline{\underline{H_R}}(\omega) + i\underline{\underline{H_I}}(\omega)$, also called the "complex spectral signature" of the saturated porous material. $\underline{\underline{H}}$, as well as $\underline{\underline{H_R}}$ and $\underline{\underline{H_I}}$, are symmetric. Moreover, $\underline{\underline{H_R}}$ and $\underline{\underline{H_I}}$ are definite positive. Thus, they can be diagonalized, but their principal directions can be theoretically different. They can be easily expressed as a function of the *microscopic* fluid field velocity $\underline{v^r}$ which is kinematically admissible, solution of:

$$\frac{1}{|\Omega|} \int_{\Omega_f} v_i^r \, d\Omega = (\delta_{1r}, \delta_{2r}, \delta_{3r})^T = \underline{V^r} .$$

where $\underline{V^r}$ is the unit macroscopic filtration velocity. The formulae are (e.g., Auriault, 1980),

$$H_{1_{qr}} = \frac{1}{|\Omega|} \int_{\Omega_f} \eta' \, v^r_{k,yj} \, \overline{v^q_{k,yj}} \, d\Omega = \frac{1}{|\Omega} \int_{\Omega_f} \eta' \, v^q_{k,yj} \, \overline{v^r_{k,yj}} \, d\Omega , \tag{20.a}$$

$$H_{2_{qr}} = \frac{1}{|\Omega|}\int_{\Omega_f} \omega\,\rho_f\, v_k^r\,\overline{v_k^q}\,d\Omega = \frac{1}{|\Omega|}\int_{\Omega_f} \omega\,\rho_f v_k^q\,\overline{v_k^r}\,d\Omega, \tag{20.b}$$

where η is the saturant fluid dynamic viscosity ($\eta' = \epsilon^2\eta$), and $\overline{v^r}$ denotes the complex conjugate.

Such a definition emphasizes the dissipative and inertial character of $\underline{\underline{H_R}}(\omega)$ and $\underline{\underline{H_I}}(\omega)$, respectively, as well as their dependence with respect to the frequency and the pore geometry through the *microscopic* field velocity of the fluid.

Partial stresses Formulation

For the complete isotropic case, following the initial work of Biot (1956a, b), the constitutive equations are very often written in terms of the partial stress in the solid $\underline{\underline{\sigma}}$ and the partial stress in the saturant fluid $s = -\tilde{\varphi}p$ such as $\underline{\underline{\Sigma}} = \underline{\underline{\sigma}} + s\underline{\underline{I}}$ ($\underline{\underline{I}}$ being the unit tensor). The viscous stress of the saturant fluid ($S_{ij} = \tilde{\varphi}\left\{\lambda_f \nabla\cdot\underline{U} + \eta(U_{i,j} + U_{j,i})\right\}$) is, for such a first order description, equal to $0(\epsilon s)$. It is then negligible with respect to the tension at the macroscopic scale. Physically, this means that flow exists only when the local gradient of the viscous stress is less (or of the same order of magintude) than the microscospic gradient of the pressure (if not, the saturant fluid is motionless with respect to the skeleton). With the uniform porosity assumption, the total and partial stresses formulations are strictly equivalent. Furthermore, the latter presents the advantage of emphasizing the symmetry between both constituents and it allows simple physical interpretation. After some straightforward algebraic manipulations, and introducing a frequency-time dependence of the form $e^{i\omega t}$, equations (6) to (9) respectively become:

$$\underline{\underline{\sigma}} = \underline{\underline{d}}\cdot\underline{\underline{e}} + \underline{\underline{Q}}\,\nabla\cdot\underline{U}\,, \tag{21}$$

$$\nabla\cdot\underline{\underline{\sigma}} = -\omega^2\left\{\underline{\underline{\gamma_{11}}}(\omega)\,\underline{u} + \underline{\underline{\gamma_{12}}}(\omega)\,\underline{U}\right\}\,, \tag{22}$$

$$s = \underline{\underline{Q}}\cdot\underline{\underline{e}} + \tilde{\mathcal{R}}\,\nabla\cdot\underline{U}\,, \tag{23}$$

$$\nabla s = -\omega^2\left\{\underline{\underline{\gamma_{12}}}(\omega)\,\underline{u} + \underline{\underline{\gamma_{22}}}(\omega)\,\underline{U}\right\}\,, \tag{24}$$

with

$$\underline{\underline{d}} = \underline{\underline{c}} + \frac{1}{\beta}\left(\underline{\underline{\alpha}} - \tilde{\varphi}\underline{\underline{I}}\right)\left(\underline{\underline{\alpha}} - \tilde{\varphi}\underline{\underline{I}}\right) \tag{25}$$

$$\Longleftrightarrow\ d_{klmn} = c_{klmn} + \frac{1}{\beta}(\alpha_{kl} - \tilde{\varphi}\delta_{kl})(\alpha_{mn} - \tilde{\varphi}\delta_{mn})\,, \tag{26}$$

$$\underline{\underline{Q}} = \tilde{\varphi}\left(\underline{\underline{\alpha}} - \tilde{\varphi}\underline{\underline{I}}\right)/\beta\,, \tag{27}$$

$$\tilde{\mathcal{R}} = \tilde{\varphi}^2/\beta\,, \tag{28}$$

and

$$\underline{\underline{\gamma_{ll}}}(\omega) = \underline{\underline{\rho_{ll}}}(\omega) - \frac{i}{\omega}\,\underline{\underline{b}}(\omega), \quad (l=1,2)\,, \tag{29}$$

$$\underline{\underline{\gamma_{12}}}(\omega) = \underline{\underline{\rho_{12}}}(\omega) + \frac{i}{\omega}\,\underline{\underline{b}}(\omega)\,, \tag{30}$$

where

$$\underline{\underline{b}}(\omega) = \tilde{\varphi}^2\,\underline{\underline{H_R}}(\omega)\,, \tag{31}$$

$$\underline{\underline{\rho_{22}}}(\omega) = \frac{\tilde{\varphi}^2}{\omega}\,\underline{\underline{H_I}}(\omega)\,, \tag{32}$$

$$\underline{\underline{\rho_{12}}}(\omega) = \tilde{\varphi}\rho_f\,\underline{\underline{I}} - \underline{\underline{\rho_{22}}}(\omega)\,, \tag{33}$$

$$\underline{\underline{\rho_{11}}}(\omega) = (1-\tilde{\varphi})\rho_s\underline{\underline{I}} - \underline{\underline{\rho_{12}}}(\omega)\,. \tag{34}$$

Equations (21) and (22) represent the dynamics equation and the macroscopic behavior law for the solid phase while equations (23) and (24) refer to the saturant fluid. The dynamic equations (22) and (24) yield the two types of forces through which the two phases are coupled.

The first force is characterized by the term $i\omega\,\underline{\underline{b}}(\omega)(\underline{U}-\underline{u})$ related to the fluid-solid relative displacement. From the definitions of $\underline{\underline{b}}(\omega)$ (equ. (31)) and $\underline{\underline{H_R}}(\omega)$, it is seen to be a viscous type force. The resulting dissipated power $\mathcal{D}$ is:

$$\mathcal{D} = \frac{1}{2}\tilde{\varphi}^2\,H_{R_{ij}}\,(\dot{U}_i - \dot{u}_i)\cdot\overline{(\dot{U}_j - \dot{u}_j)}\,.$$

Such a formula can be directly obtained by integration over a period of the dissipated power per unit volume defined at the microscopic scale (at the first order) as the product of the strain tensors times the viscous stresses (Boutin, 1987).

The second force is inertial as it can be seen from the acceleration terms (proportional to ω^2). In addition to the classical inertial terms $(1-\tilde{\varphi})\rho_s\,\underline{u}$ and $\tilde{\varphi}\rho_f\,\underline{U}$, respectively for the solid and the fluid, each equation exhibits a coupling term associated with the relative acceleration between the two phases, affected by a tensorial mass equal to $\underline{\underline{\rho_{12}}}(\omega)$. In the principal axes of $\underline{\underline{H_I}}(\omega)$, it can be shown (Auriault, 1980) that each diagonal term verifies the inequality:

$$\frac{\tilde{\varphi}}{\omega}\frac{H_{I_{ii}}(\omega}{\rho_f} \geq 1\,.$$

Such a relation points out an added mass effect as the saturant fluid apparent density ($\rho_{22_{ii}}(\omega) = \tilde{\varphi}\rho_f\cdot\frac{\tilde{\varphi}}{\omega}\frac{H_{I_{ii}}}{\rho_f}$) is greater than (or equal to) the true density ($\tilde{\varphi}\rho_f$). As another consequence, $\rho_{12_{ii}} \leq 0$.

The existence of two types of forces leads to two separated frequency domains for the behavior of the saturated porous formation along each principal direction. In the "low frequency" domain, the viscous force is predominant while in the "high frequency" domain, the inertial force plays the major role. Similarly to the complete isotropic case (e.g., Schmitt, 1986a), the forces are of the same order of magnitude at a *critical* frequency

$$f_{c_l} = \frac{\eta \tilde{\varphi}^2}{2\pi \tilde{k}_l \rho_{22_l}(0)} , \tag{35}$$

where $\tilde{k}_l$ is the intrinsic permeability in the lth principal direction.

The total stresses formulation occured to be theoretically very powerful. For example, it leads to simple formulae when defining the Green's function and associated sources in an isotropic saturated porous formation (Boutin et al., 1987). Nevertheless, the partial stresses formulation is used hereinafter. The formulae presented are totally general. We limit the derivations to the tranverse isotropy situation because of our interest in acoustic and shear wave logging (see Part II). One can easily solve the equations for orthotropic saturated porous media.

Transversely Isotropic Saturated Porous Formation

The generic expression "transversely isotropic saturated porous" formation implies that either only the skeleton, or the permeability tensor, or both of them are transversely isotropic. Using the abberviated subscripts notation as described by Auld (1973), the stiffness tensor of a transversely isotropic skeleton has five independent elastic constants and can be written as:

$$\begin{pmatrix} c_{11} & c_{12} & c_{13} & 0 & 0 & 0 \\ c_{12} & c_{11} & c_{13} & 0 & 0 & 0 \\ c_{13} & c_{13} & c_{33} & 0 & 0 & 0 \\ 0 & 0 & 0 & c_{44} & 0 & 0 \\ 0 & 0 & 0 & 0 & c_{44} & 0 \\ 0 & 0 & 0 & 0 & 0 & c_{66} \end{pmatrix} , \tag{36}$$

with $c_{66} = (c_{11} - c_{12})/2$, and the stability conditions that ensure positive definite strain energy, i.e., $c_{44} > 0$, $c_{66} > 0$, $c_{11} - c_{66} > 0$, and $c_{33}(c_{11} - c_{66}) > c_{13}^2$.

With the abbreviated subscripts notation, the elastic tensor $\underline{\underline{\alpha}}$ becomes a vector whose elements are

$$\alpha_1 = \alpha_2 = 1 - \frac{1}{3K_s}(c_{11} + c_{12} + c_{13}), \text{ and } \alpha_3 = 1 - \frac{1}{3K_s}(2c_{13} + c_{33}) . \tag{37}$$

The constant β becomes:

$$\beta = \frac{1 - \tilde{\varphi}}{K_s} + \frac{\tilde{\varphi}}{K_f} - \frac{1}{9K_s^2}(2c_{11} + 2c_{12} + 4c_{13} + c_{33}) , \tag{38}$$

so that the elements of the "vector" $\underline{Q}$ are

$$Q_1 = Q_2 = \tilde{\varphi}\,(\alpha_1 - \tilde{\varphi})\,/\beta, \quad \text{and} \quad Q_3 = \tilde{\varphi}\,(\alpha_3 - \tilde{\varphi})\,/\beta\,. \tag{39}$$

The tensor $\underline{\underline{d}}$ has the same structure as the stiffness tensor $\underline{\underline{c}}$, its elements being:

$$d_{kl} = c_{kl} + \frac{1}{\beta}(\alpha_k - \tilde{\varphi})(\alpha_l - \tilde{\varphi})\,, \tag{40}$$

with $d_{66} = \dfrac{1}{2}(d_{11} - d_{12})$.

The above formulae slightly differ from those evaluated by Yew and Weng (1987) who used a composite material theory and the total stress formulation.

Because of the assumption (13), the complex permeability tensor $\underline{\underline{K}}(\omega)$ is diagonal in a singular basis, i.e.:

$$\underline{\underline{K}}(\omega) = \begin{pmatrix} K_1(\omega) & 0 & 0 \\ 0 & K_1(\omega) & 0 \\ 0 & 0 & K_3(\omega) \end{pmatrix}\,. \tag{41}$$

For each l principal direction, the complex dynamic permeability can be evaluated with simple pore geometries. One of the most usual is the unidirectional cylindrical duct model for which the Navier-Stockes equations can be directly used to obtain $K_l(\omega)$ at the macroscopic scale(e.g., Schmitt, 1986a):

$$K_l(\omega) = -\frac{\tilde{\varphi}}{i\omega\rho_f} J_2\left\{ia_l\left(\frac{i\omega\,\rho_f}{\mu}\right)^{\frac{1}{2}}\right\} / J_0\left\{ia_l\left(\frac{i\omega\,\rho_f}{\mu}\right)^{\frac{1}{2}}\right\}\,, \tag{42}$$

where J_j are Bessel functions of the first kind of the jth order. The characteristic pore dimension a_l (i.e., the duct radius) is deduced from Darcy's law:

$$\lim_{\omega\to 0} b_l(\omega) = \eta\,\tilde{\varphi}^2/\tilde{k}_l = 8\eta\tilde{\varphi}/a_l^2 \implies a_l^2 = 8\tilde{k}_l/\tilde{\varphi}\,, \tag{43}$$

where, as already stated, $\tilde{k}_l$ is the intrinsic permeability in the lth direction.

Such a model enhances the diphasic effects because $\rho_{22_l}(\infty) = \tilde{\varphi}\rho_f$ but disagrees with experimental measurements performed with isotropic saturated porous materials (e.g., Johnson et al., 1982) which show that $\rho_{22}(\infty)/(\tilde{\varphi}\rho_f) > 1$. Biot (1956a, b) already knew the "hiatus" of the unidirectional cylindrical model and introduced a tortuosity factor $\tilde{\tau}$. This factor expresses the average ratio of total arc length travelled to the actual straight line progress when pursuing the shortest possible connected path through the pore space. Hence, for each principal direction,

$$\tilde{\tau}_l \geq 1\,. \tag{44}$$

Introducing this factor through the pore radius a_l which becomes $\sqrt{\tilde{\tau}_l}a_l$, the complex spectral signature $H_l(\omega)$ is multiplied by the tortuosity, so that the viscous and mass coupling coefficients become:

$$b_l(\omega, \tilde{\tau}_l) = \tilde{\tau}_l\tilde{\varphi}^2 H_{R_l}(\omega) , \tag{45}$$

$$\rho_{22_l}(\omega, \tilde{\tau}_l) = \tilde{\tau}_l\tilde{\varphi}^2 H_{I_l}(\omega)/\omega , \tag{46}$$

$$\rho_{12_l}(\omega, \tilde{\tau}_l) = \tilde{\varphi}\rho_f - \rho_{22_l}(\omega, \tilde{\tau}_l) , \tag{47}$$

$$\rho_{11_l}(\omega, \tilde{\tau}_l) = (1-\tilde{\varphi})\rho_s - \rho_{12_l}(\omega, \tilde{\tau}_l) . \tag{48}$$

The zero frequency limit of the viscous coupling coefficient remains unchanged whatever the tortuosity in accordance with no variation of the intrinsic permeability $\tilde{k}_l$, while the high frequency limit of the dimensionless mass coupling coefficient can now be greater than one. The characteristic frequency (equ.(35)) is divided by the tortuosity which thus leads to a shift toward lower frequencies of the occurence of the inertial effects. It can be easily shown that the Kramers-Koening relations (equ. (16) to (19)) are still verified, whatever the tortuosity value in each principal direction.

Although such a factor presents the advantage to allow relatively more accurate numerical simulations, it is not sufficient to fully describe the flow geometry. Such a limitation can be seen from the high frequency limit calculations performed by Borne (1983) using the plane boundary layer theory (i.e., the fluid is perfect but with a skin (viscosity) effects at the pore wall): the complex spectral signature is function of *two shape tensors*. The limitation of the tortuosity factor is even emphasized by the fact that these calculations do not take into account any constriction of the pore space and the relevant effects on the microscopic field of the fluid velocity.

Isotropic Saturated Porous Formation

The formulae for an isotropic skeleton, are easy to deduce. Denoting λ_b, μ_b the Lamé coefficients of the skeleton and K_b the associated bulk modulus, one obtains:

- for the stiffness tensor $\underline{c}$:

$$\begin{aligned} c_{12} &= c_{13} = \lambda_b , \\ c_{44} &= c_{66} = \mu_b = N , \\ c_{11} &= c_{33} = \lambda_b + 2\mu_b ; \end{aligned} \tag{49}$$

- for the elastic tensor $\underline{\alpha}$:

$$\alpha_1 = \alpha_3 = \alpha = 1 - \frac{K_b}{K_s} ; \tag{50}$$

- for the compressibility coefficient β:

$$\beta = \frac{1-\tilde{\varphi}}{K_s} + \frac{\tilde{\varphi}}{K_f} - \frac{K_b}{K_s^2} = \frac{\alpha-\tilde{\varphi}}{K_s} + \frac{\tilde{\varphi}}{K_f} \; ; \tag{51}$$

- for the elastic constant $\tilde{\mathcal{R}}$:

$$\tilde{\mathcal{R}} = \frac{\tilde{\varphi}^2 K_s}{1-\tilde{\varphi}-\dfrac{K_b}{K_s}+\tilde{\varphi}\dfrac{K_s}{K_f}} = \tilde{R} \; ; \tag{52}$$

- for the tensor $\underline{\underline{Q}}$:

$$Q_1 = Q_3 = \frac{\tilde{\varphi} K_s \left(1-\tilde{\varphi}-\dfrac{K_b}{K_s}\right)}{1-\tilde{\varphi}-\dfrac{K_b}{K_s}+\tilde{\varphi}\dfrac{K_s}{K_f}} = Q \; ; \tag{53}$$

- and for the tensor $\underline{\underline{d}}$:

$$d_{12} = d_{13} = \frac{(1-\tilde{\varphi})\left(1-\tilde{\varphi}-\dfrac{K_b}{K_s}\right) K_s + \tilde{\varphi}\dfrac{K_s}{K_f} K_b}{1-\tilde{\varphi}-\dfrac{K_b}{K_s}+\tilde{\varphi}\dfrac{K_s}{K_f}} - \frac{2}{3}\mu_b = A \; , \tag{54.a}$$

$$d_{11} = d_{33} = A + 2N = P \; , \tag{54.b}$$

$$d_{44} = d_{66} = N \; . \tag{54.c}$$

The dynamics equations (21) and (23) become (with $\varepsilon = \nabla \cdot \underline{U}$):

$$\begin{array}{rcl} \sigma_{ij} & = & 2N e_{ij} + (A\, e + Q\, \varepsilon)\, \delta_{ij} \; , \\ s\, \delta_{ij} & = & \left(Q\, e + \tilde{R}\, \varepsilon\right) \delta_{ij} \; . \end{array} \tag{55}$$

For an isotropic fluid distribution, the complex permeability tensor reduces to $\underline{\underline{K}}(\omega) = K(\omega)\underline{\underline{I}}$ so that the equations of motion (22) and (24) are given by:

$$\begin{array}{rcl} \partial_j \sigma_{ij} & = & -\omega^2(\gamma_{11}\, u_i + \gamma_{12}\, U_i) \; , \\ \partial_i s & = & -\omega^2(\gamma_{12}\, u_i + \gamma_{22}\, U_i) \; . \end{array} \tag{56}$$

where the variables γ_{kl} are given by the equations (29) and (30) dropping the tensor notation as well as for the viscous and mass coupling coefficient (equ. (31) to (34)). Equations (45) to (48) can also be used for these last, dropping the index which refers

to a principal direction. The tortuosity then corresponds to the distribution of non interconnected straight cylindrical ducts.

These are the usual equations for an isotropic saturated porous material. Compared to those of Biot (1956a, b), the mass coupling coefficients (ρ_{ij}) are frequency dependent, interrelated with the viscous coupling coefficient ($b(\omega)$), and pore geometry dependent.

Elastic Formation

An elastic formation corresponds to a zero porosity porous formation. The constitutive equations are then (from equations (21) to (24), noting ρ the density):

$$\underline{\underline{\sigma}} = \underline{\underline{c}} \cdot \underline{\underline{\epsilon}} \tag{57}$$

$$\nabla \cdot \underline{\underline{\sigma}} = -\omega^2 \rho \, \underline{u} \, . \tag{58}$$

The stiffness tensor $\underline{\underline{c}}$ is given by the equation (36) when the formation is transversely isotropic. Following Backus (1962), each element can be evaluated when the formation is considered as resulting from the average properties of two different solids whose thicknesses are small with respect to the wavelength. When both solids are transversely isotropic associated with a fraction h_i (with $h_1 + h_2 = 1$), one has:

$$\begin{aligned}
c_{11} &= h_1 \left(c_{11_1} - \frac{c_{13_1}^2}{c_{33_1}} \right) h_2 \left(c_{11_2} - \frac{c_{13_2}^2}{c_{33_2}} \right) + \left(\frac{h_1}{c_{33_1}} + \frac{h_2}{c_{33_2}} \right)^{-1} \left(h_1 \frac{c_{13_1}}{c_{33_1}} + h_2 \frac{c_{13_2}}{c_{33_2}} \right)^2 , \\
c_{13} &= \left(\frac{h_1}{c_{33_1}} + \frac{h_2}{c_{33_2}} \right)^{-1} \left(h_1 \frac{c_{13_1}}{c_{33_1}} + h_2 \frac{c_{13_2}}{c_{33_2}} \right) , \\
c_{33} &= \left(\frac{h_1}{c_{33_1}} + \frac{h_2}{c_{33_2}} \right)^{-1} , \\
c_{44} &= \left(\frac{h_1}{c_{44_1}} + \frac{h_2}{c_{44_2}} \right)^{-1} , \\
c_{66} &= h_1 \, c_{66_1} + h_2 \, c_{66_2} , \\
\rho &= h_1 \, \rho_1 + h_2 \, \rho_2
\end{aligned} \tag{59}$$

These formulae also apply for isotropic constituents using equations (49). Equivalent transversely isotropic layers can also be obtained for periodically stratified media (e.g., Schoenberg, 1983).

When the formation is isotropic, the constitutive equations (57) and (58) still hold true, the elements of the tensor $\underline{\underline{c}}$ being given by the equations (49).

WAVENUMBERS EQUATIONS

In order to obtain the wavenumbers equations, the choice of a coordinates system and of the form of the wave potentials has to be made. Usually, the solutions are searched in terms of plane waves and the solutions are presented as a function of the slowness (i.e., the inverse of velocity): the Christoffel equations (e.g., Auld, 1973). For consistency with the applications (see Part II), we consider the well logging geometry. Defining a cylindrical coordinates system as (r, θ, z), the model consists of fluid-filled borehole extending to infinity in the z direction embedded in a (radially layered) formation. Constructing the acoustic field in a borehole due to a multipole *point* source (e.g., Schmitt and Cheng, 1987), the expression of the displacement potential in the borehole fluid with respect to a nth order multipole point source is given in the frequency-axial wavenumber domain by:

$$\Phi_1^{(n)} = \frac{1}{n!}\left(\frac{kp_1 R_0}{2}\right)^n \tilde{A_1}^{(n)} I_n(kp_1\, r)\cos[n(\theta-\theta_0)]e^{ikz}e^{i\omega t}\,, \qquad (60)$$

where k is the axial wavenumber, and ω is the angular frequency. $kp_1^2 = k^2 - \omega^2/cp_1^2$, is the radial wavenumber with respect to the bore fluid velocity cp_1. $\tilde{A_1}^{(n)}$ is a weighting coefficient function of k and ω. R_0 is the radius over which the point sources are distributed, and θ_0 is an arbitrary angle of reference. I_n denotes the nth order modified Bessel function of the first kind.

We first derive the wavenumbers equations for a complete transversely isotropic saturated porous material. The case of the only transversely isotropic permeability is then discussed, followed by the complete isotropic situation. The case of an elastic formation, either transversely isotropic or isotropic, is also presented.

Transversely Isotropic Saturated Porous Formation

For clarity, we hereafter only present the principles of the calulations. The detailed derivation is given in the Appendix. First, the stress-strain relations (Equ. (21) and (23)) are written in the cylindrical coordinates system, using the knwon formuale for the strain-displacement relations in each phase (e.g., Achenbach, 1973). These formuale are then introduced into the equations of motion (22) and (24) where the divergence stress operator has been also expanded in the cylindrical coordinates system. The resulting six equations are function of the only components of the displacement vectors in each phase and of the coefficients of the transversely isotropic saturated porous formation.

In order to find the wavenumbers singular values, both displacement vectors in the solid and liquid phases are separated into their compressional, and vertically and

horizontally polarized shear components:

$$\begin{aligned} \underline{u}^{(n)} &= \nabla \cdot \Phi_s^{(n)} + \nabla \times \left(\Psi_s^{(n)} \underline{z}\right) + \nabla \times \nabla \times \left(\Gamma_s^{(n)} \underline{z}\right) , \\ \underline{U}^{(n)} &= \nabla \cdot \Phi_f^{(n)} + \nabla \times \left(\Psi_f^{(n)} \underline{z}\right) + \nabla \times \nabla \times \left(\Gamma_f^{(n)} \underline{z}\right) , \end{aligned} \tag{61}$$

where the subscripts s and f refer to the solid and the saturant fluid, respectively. $\Phi_s^{(n)}$ and $\Phi_f^{(n)}$ are compressional potentials; $\underline{z}$ is the unit vector in the z direction. $\Psi_s^{(n)}$ and $\Psi_f^{(n)}$ are horizontally polarized shear potentials (SH wave), while $\Gamma_s^{(n)}$ and $\Gamma_f^{(n)}$ are vertically polarized shear potentials (SV wave) with

$$\nabla \cdot \left(\Psi_s^{(n)} \underline{z}\right) = \nabla \cdot \left(\Psi_f^{(n)} \underline{z}\right) = \nabla \cdot \left(\Gamma_s^{(n)} \underline{z}\right) = \nabla \cdot \left(\Gamma_f^{(n)} \underline{z}\right) = 0 .$$

Denoting q the singular radial wavenumber, a suitable solution within the well logging geometry is:

for the solid,

$$\begin{aligned} \Phi_s^{(n)} &= \tilde{A}_s^{(n)} I_n(q\,r)\, e^{ikz} \cos n\theta , \\ \Psi_s^{(n)} &= \tilde{C}_s^{(n)} I_n(q\,r)\, e^{ikz} \sin n\theta , \\ \Gamma_s^{(n)} &= \tilde{E}_s^{(n)} I_n(q\,r)\, e^{ikz} \cos n\theta ; \end{aligned} \tag{62}$$

and for the fluid,

$$\begin{aligned} \Phi_f^{(n)} &= \tilde{A}_f^{(n)} I_n(q\,r)\, e^{ikz} \cos n\theta , \\ \Psi_f^{(n)} &= \tilde{C}_f^{(n)} I_n(q\,r)\, e^{ikz} \sin n\theta , \\ \Gamma_f^{(n)} &= \tilde{E}_f^{(n)} I_n(q\,r)\, e^{ikz} \cos n\theta . \end{aligned} \tag{63}$$

In the above equations, $q^2 = k^2 - \omega^2/c_w^2$, where c_w denotes a body wave velocity, and $\tilde{A}_s^{(n)}$, $\tilde{C}_s^{(n)}$, $\tilde{E}_s^{(n)}$, $\tilde{A}_f^{(n)}$, $\tilde{C}_f^{(n)}$, and $\tilde{E}_f^{(n)}$ are weighting coefficients, function of the axial wavenumber k and the angular frequency ω. The temporal dependence of the form $e^{i\omega t}$ has already been taken into account and is then understood. Compared to the exact solutions given in equation (60), the term $\dfrac{1}{2^n\, n!}(kp_1\, R_0)^n$ has been omitted and θ_0 has been set to zero, without loosing any generality. The function considered is not unique. One may take instead a modified Bessel function of the second kind of the nth order (i.e., K_n), a Bessel function of the first kind of the nth order (i.e., J_n), or Hankel functions of the nth order (i.e., $H_n^{(1)}$, $H_n^{(2)}$). The choice of another geometry would have also led to other possible solutions.

With these decompositions, the "expanded" equations of motion can be written in a matrix form:

$$\underline{\underline{\tilde{Z}}}\left(\tilde{A}_s^{(n)}, \tilde{C}_s^{(n)}, \tilde{E}_s^{(n)}, \tilde{A}_f^{(n)}, \tilde{C}_f^{(n)}, \tilde{E}_f^{(n)}\right)^T = (0, 0, 0, 0, 0, 0)^T \ , \tag{64}$$

where ^{T} denotes the transpose and $\underline{\underline{\tilde{Z}}}$ is a 6x6 complex matrix whose elements, function of the Bessel functions, are given in the Appendix.

The singular values are obtained by solving the equation Det $\left(\underline{\underline{\tilde{Z}}}\right) = 0$.

SH wave

The expression of Det $\left(\underline{\underline{\tilde{Z}}}\right)$ can be greatly simplified by performing some algebraic manipulations (see Appendix) which yield:

$$\tilde{C}_f^{(n)} = -\frac{\gamma_{12}^H}{\gamma_{22}^H}\tilde{C}_s^{(n)} = \chi^H \tilde{C}_s^{(n)} \ . \tag{65}$$

This relation is identical to the one obtained in the isotropic case (e.g., Schmitt, 1985; 1986a). It emphasizes that the fluid does not support any shear displacements but affects the *SH* wave through inertial effects.

The corresponding radial wavenumber is:

$$q^2 = k s_H^2 = \frac{d_{44}k^2 - \omega^2\left(\gamma_{11}^H - \frac{\gamma_{12}^{H^2}}{\gamma_{22}^H}\right)}{d_{66}} \ . \tag{66}$$

Only the horizontal viscous and mass coupling coefficients (i.e., the horizontal permeability) play a role.

Quasi body waves

The remaining system to be solved is then of the fourth order:

$$\underline{\underline{\tilde{Z}}}\left(\tilde{A}_s^{(n)}, \tilde{E}_s^{(n)}, \tilde{A}_f^{(n)}, \tilde{E}_f^{(n)}\right)^T = 0 \ , \tag{67}$$

where the elements ζ_{kl} of the 4x4 complex matrix $\underline{\underline{\tilde{Z}}}$ are now independent from the Bessel functions (see Appendix). As previously, the remaining singular radial wavenumbers values are obtained by solving the equation Det $\left(\underline{\underline{\tilde{Z}}}\right) = 0$.

Any algebraic manipulation does not lead to any more simple form of the determinant which has to be expanded. The resulting equations is of the order 10 in q with a common factor of the form $\omega^4 \{q^2 - k^2\}^2$. The remaining equation is of the third degree in q^2 and can be written as

$$\begin{aligned} q^6\,\Xi_1 \;&+\; q^4\,\{\,\Xi_2\,\omega^2 + \Xi_3\,k^2\} + q^2\,\{\Xi_4\,\omega^4 + \Xi_5\,k^4 + \Xi_6\,\omega^2\,k^2\} \\ &+\; \Xi_7\,\omega^6 + \Xi_8\,\omega^4\,k^2 + \Xi_9\,\omega^2\,k^4 + \Xi_{10}\,k^6 = 0\;, \end{aligned} \tag{68.a}$$

where

$$\Xi_1 = d_{44}\,\gamma_{22}^V\,\left(d_{11}\,\tilde{\mathcal{R}} - Q_1^2\right)\;, \tag{68.b}$$

$$\Xi_2 = \left(d_{11}\,\tilde{\mathcal{R}} - Q_1^2\right)\left(\gamma_{11}^V\,\gamma_{22}^V - \gamma_{12}^{V^2}\right) + d_{44}\,\gamma_{22}^V\left(d_{11}\,\gamma_{22}^H + \tilde{\mathcal{R}}\,\gamma_{11}^H - 2\,Q_1\gamma_{12}^H\right)\;, \tag{68.c}$$

$$\begin{aligned} \Xi_3 \;&=\; -d_{44}\,\gamma_{22}^H\left(d_{11}\,\tilde{\mathcal{R}} - Q_1^2\right) + \gamma_{22}^V\,[\,2\,d_{44}\left(d_{13}\,\tilde{\mathcal{R}} - Q_1\,Q_3\right) \\ &+\; d_{13}\left(d_{13}\,\tilde{\mathcal{R}} - 2\,Q_1\,Q_3\right) - d_{33}\left(d_{11}\,\tilde{\mathcal{R}} - Q_1^2\right) + d_{11}\,Q_3^2\,]\;, \end{aligned} \tag{68.d}$$

$$\Xi_4 = \left(d_{11}\,\gamma_{22}^H + \tilde{\mathcal{R}}\,\gamma_{11}^H - 2\,Q_1\,\gamma_{12}^H\right)\left(\gamma_{11}^V\,\gamma_{22}^V - \gamma_{12}^{V^2}\right) + d_{44}\,\gamma_{22}^V\left(\gamma_{11}^H\,\gamma_{22}^H - \gamma_{12}^{H^2}\right)\;, \tag{68.e}$$

$$\begin{aligned} \Xi_5 \;&=\; d_{44}\,\gamma_{22}^V\left(d_{33}\,\tilde{\mathcal{R}} - Q_3^2\right) + \gamma_{22}^H\,[\,-2\,d_{44}\left(d_{13}\,\tilde{\mathcal{R}} - Q_1\,Q_3\right) \\ &-\; d_{13}\left(d_{13}\,\tilde{\mathcal{R}} - 2\,Q_1\,Q_3\right) + d_{33}\left(d_{11}\,\tilde{\mathcal{R}} - Q_1^2\right) - d_{11}\,Q_3^2\,]\;, \end{aligned} \tag{68.f}$$

$$\begin{aligned} \Xi_6 \;&=\; -d_{44}\,\tilde{\mathcal{R}}\left(\gamma_{11}^V\,\gamma_{22}^V - \gamma_{12}^{V^2} + \gamma_{11}^H\,\gamma_{22}^H - \gamma_{12}^{H^2}\right) \\ &-\; \gamma_{11}^H\,\gamma_{22}^V\left(d_{33}\,\tilde{\mathcal{R}} - Q_3^2\right) - \gamma_{11}^V\,\gamma_{22}^H\left(d_{11}\,\tilde{\mathcal{R}} - Q_1^2\right) \\ &+\; 2\,\gamma_{12}^H\,\gamma_{12}^V\left[\tilde{\mathcal{R}}\,(d_{44} + d_{13}) - Q_1\,Q_3\right] \\ &-\; 2\,\gamma_{12}^H\,\gamma_{22}^V\,[Q_3\,(d_{44} + d_{13}) - Q_1\,d_{33}] \\ &-\; 2\,\gamma_{12}^V\,\gamma_{22}^H\,[Q_1\,(d_{44} + d_{13}) - Q_3\,d_{11}] \\ &+\; \gamma_{22}^H\,\gamma_{22}^V\,(2\,d_{13}\,d_{44} - d_{11}\,d_{33} + d_{13}^2)\;, \end{aligned} \tag{68.g}$$

$$\Xi_7 = \left(\gamma_{11}^H\,\gamma_{22}^H - \gamma_{12}^{H^2}\right)\left(\gamma_{11}^V\,\gamma_{22}^V - \gamma_{12}^{V^2}\right)\;, \tag{68.h}$$

$$\Xi_8 = -\left(\gamma_{11}^H\,\gamma_{22}^H - \gamma_{12}^{H^2}\right)\left(d_{33}\,\gamma_{22}^V + \tilde{\mathcal{R}}\gamma_{11}^V - 2\,Q_3\,\gamma_{12}^V\right) - d_{44}\,\gamma_{22}^H\left(\gamma_{11}^V\,\gamma_{22}^V - \gamma_{12}^{V^2}\right)\;, \tag{68.i}$$

$$\Xi_9 = \left(\gamma_{11}^H\,\gamma_{22}^H - \gamma_{12}^{H^2}\right)\left(d_{33}\,\tilde{\mathcal{R}} - Q_3^2\right) + d_{44}\,\gamma_{22}^H\left(d_{33}\,\gamma_{22}^V + \tilde{\mathcal{R}}\,\gamma_{11}^V - 2\,Q_3\,\gamma_{12}^V\right)\;, \tag{68.j}$$

and

$$\Xi_{10} = -d_{44}\,\gamma_{22}^H\left(d_{33}\,\tilde{\mathcal{R}} - Q_3^2\right)\;. \tag{68.k}$$

This equation has always three independent solutions corresponding to quasi P_1, P_2, and SV waves. They are, of course, independent from the cylindrical geometry chosen at the very first beginning.

None of the scalar and vector potentials relative to the quasi-compressional and quasi-SV waves is solution of the equations of motion. This is due to the coupling between the body waves on which is superimposed to the coupling between the solid and liquid phases which leads to the existence of the two compressional waves. All three waves have a compressional part and a rotational part. Taking into account the additional coupling between the solid and the liquid phases, the wave potentials can be expressed, in their most general form, as:

- for both quasi P_i-wave:

$$\begin{aligned} \Phi_s^{(n)Pi} &= \tilde{A}_i^{(n)}\, F(kp_{ti},\, k,\, \omega)\,, \\ \Gamma_s^{(n)Pi} &= \mathcal{Y}_1^{Pi}\, \Phi_s^{(n)Pi}\,, \\ \Phi_f^{(n)Pi} &= \mathcal{Y}_2^{Pi}\, \Phi_s^{(n)Pi}\,, \\ \Gamma_f^{(n)Pi} &= \mathcal{Y}_3^{Pi}\, \Phi_s^{(n)Pi}\,; \end{aligned} \tag{69.a}$$

- and, for the quasi SV-wave:

$$\begin{aligned} \Phi_s^{(n)SV} &= \mathcal{Y}_1^{SV}\, \Gamma_s^{(n)SV}\,, \\ \Gamma_s^{(n)SV} &= \tilde{E}^{(n)}\, F(ks_V,\, k\,\omega)\,, \\ \Gamma_f^{(n)SV} &= \mathcal{Y}_2^{SV}\, \Gamma_s^{(n)SV}\,, \\ \Gamma_f^{(n)SV} &= \mathcal{Y}_3^{SV}\, \Gamma_s^{(n)SV}\,. \end{aligned} \tag{69.b}$$

In the above equations, $\mathcal{Y}_1^{P1}$, $\mathcal{Y}_1^{P2}$, $\mathcal{Y}_1^{SV}$, $\mathcal{Y}_2^{P1}$, $\mathcal{Y}_2^{P2}$, $\mathcal{Y}_2^{SV}$, $\mathcal{Y}_3^{P1}$, $\mathcal{Y}_3^{P2}$, and $\mathcal{Y}_3^{SV}$ denote the "constants" which expressed the coupling between the body waves and/or the two phases of the saturated porous formation. $\tilde{A}_1^{(n)}$, $\tilde{A}_2^{(n)}$, and $\tilde{E}^{(n)}$ are weighting coefficients, functions of the wavenumber k and the angular frequency ω, which can be interpreted as the transmission coefficients. $F(\nu,\, k,\, \omega)$ with $\nu = kp_{t1}$, kp_{t2}, ks_V is the function which expresses the wave propagation. It depends on the chosen geometry. In order to be consistent with the previous derivations, $F(\nu,\, k,\, \omega) = I_n(\nu\, r)e^{ikz}e^{i\omega t}$.

The final solutions for the solid and liquid phases can be expressed as:

$$\begin{aligned}
\Phi_s^{(n)} &= \Phi_s^{(n)P1} + \Phi_s^{(n)P2} + \Phi_s^{(n)SV} \,, \\
\Gamma_s^{(n)} &= \Gamma_s^{(n)P1} + \Gamma_s^{(n)P2} + \Gamma_s^{(n)SV} \,, \\
\Phi_f^{(n)} &= \Phi_f^{(n)P1} + \Phi_f^{(n)P2} + \Phi_f^{(n)SV} \,, \\
\Gamma_f^{(n)} &= \Gamma_f^{(n)P1} + \Gamma_f^{(n)P2} + \Gamma_f^{(n)SV} \,.
\end{aligned} \tag{70}$$

The "coupling" coefficients $\mathcal{Y}_1^{P1}, \mathcal{Y}_1^{SV}, \mathcal{Y}_2^{P1}, \mathcal{Y}_2^{P2}, \mathcal{Y}_2^{SV}, \mathcal{Y}_3^{P1}, \mathcal{Y}_3^{P2}, \mathcal{Y}_3^{SV}$ are evaluated using the singular equations of the quasi body waves (Equ. (67)) with the above potential decompositions. The systems to be solved are then:

-for both quasi P_i-waves:

$$\underline{\underline{\tilde{Z}}}(kp_{ti}) \left(1, \mathcal{Y}_1^{Pi}, \mathcal{Y}_2^{Pi}, \mathcal{Y}_3^{Pi}\right)^T = 0 \,, \tag{71}$$

-and for the quasi SV-wave:

$$\underline{\underline{\tilde{Z}}}(ks_V) \left(\mathcal{Y}_1^{SV}, 1, \mathcal{Y}_2^{SV}, \mathcal{Y}_3^{SV}\right)^T = 0 \,. \tag{72}$$

These systems are overdetermined. Only the first three equations need to be used, the fourth one being automatically verified. Such a method is totally general, independent from the geometry.

Transversely isotropic permeability only

When only the skeleton is isotropic, the elastic coefficients and the tensors are given by equations (49) to (54). Although still valid, the previous developments are not fully necessary. The equations of motion can be written in a tensor form:

$$\begin{aligned}
\underline{\underline{N}}\,\nabla^2 \underline{u}^{(n)} + \left(\underline{\underline{A}} + \underline{\underline{N}}\right) \nabla\nabla\cdot\underline{u}^{(n)} + \underline{\underline{Q}}\,\nabla\nabla\cdot\underline{U}^{(n)} &= -\omega^2 \left(\underline{\underline{\gamma_{11}}}\,\underline{u}^{(n)} + \underline{\underline{\gamma_{12}}}\,\underline{U}^{(n)}\right) \,, \\
\underline{\underline{Q}}\,\nabla\nabla\cdot\underline{u}^{(n)} + \underline{\underline{\tilde{R}}}\,\nabla\nabla\cdot\underline{U}^{(n)} &= -\omega^2 \left(\underline{\underline{\gamma_{12}}}\,\underline{u}^{(n)} + \underline{\underline{\gamma_{22}}}\,\underline{U}^{(n)}\right) \,,
\end{aligned} \tag{73}$$

where $\underline{\underline{A}} = A\,\underline{\underline{I}}$; $\underline{\underline{N}} = N\,\underline{\underline{I}}$; $\underline{\underline{P}} = P\,\underline{\underline{I}}$; $\underline{\underline{Q}} = Q\,\underline{\underline{I}}$; $\underline{\underline{\tilde{R}}} = \tilde{R}\,\underline{\underline{I}}$ and,

$$\underline{\underline{\gamma_{kl}}} = \begin{pmatrix} \gamma_{kl}^H & 0 & 0 \\ 0 & \gamma_{kl}^H & 0 \\ 0 & 0 & \gamma_{kl}^V \end{pmatrix} \qquad k = 1,2;\ l = 1,2 \,.$$

Introducing the potentials decomposition (Equ. (62) and (63)), and applying the curl operator, one obtains:

$$\nabla \times \underline{\Psi}_f^{(n)} = -\gamma_{22}^{H-1}\,\gamma_{12}^{H}\,\nabla \times \underline{\Psi}_s^{(n)}\,, \tag{74.a}$$

$$\nabla^2 \underline{\Psi}_s^{(n)} = -\frac{\omega^2}{N}\left(\gamma_{11}^{H} - \gamma_{12}^{H^2}\,\gamma_{22}^{H^{-1}}\right)\,, \tag{74.b}$$

$$\nabla \times \nabla \times \underline{\Gamma}_f^{(n)} = -\underline{\underline{\gamma_{22}}}^{-1}\,\underline{\underline{\gamma_{12}}}\,\nabla \times \nabla \times \underline{\Gamma}_s^{(n)}\,, \tag{74.c}$$

$$\begin{aligned}&\omega^2\,\nabla \times \left(\underline{\underline{\gamma_{11}}}\,\nabla \cdot \Phi_s^{(n)}\right) + \omega^2\,\nabla \times \left(\underline{\underline{\gamma_{12}}}\,\nabla \cdot \Phi_f^{(n)}\right)\\ &+\underline{\underline{N}}\,\nabla \times \nabla \times \nabla \times \left(\nabla^2 \underline{\Gamma}_s^{(n)}\right) + \omega^2\,\nabla \times \left\{\left(\underline{\underline{\gamma_{11}}} - \underline{\underline{\gamma_{12}}}^2\,\underline{\underline{\gamma_{22}}}^{-1}\right)\nabla \times \nabla \times \underline{\Gamma}_s^{(n)}\right\} \;=\; 0\,.\end{aligned} \tag{74.d}$$

As previously, only the SH-wave wavenumber can be solved. The remaining equations indicate the coupling between the P_1, P_2, and SV waves. Applying the divergence operator, coupled equations are also obtained. Thus, the only transversely isotropic permeability is sufficient to lead to quasi body waves. The same result is of course obtained when only the skeleton is transversely isotropic.

Isotropic Saturated Porous Formation

When both the skeleton and the permeability are isotropic, only the coupling between the two phases remains so that both compressional waves are decoupled from the shear wave. Their characteristics can be obtained either by taking the isotropic coefficients (Equ. (49) to (54)) and solving directly the equations of motion, or by factorizing the equation (68). Denoting $\mathcal{X} = k^2 - q^2$, these equations can be written as:

$$-\omega^2\,\mathcal{X}^2 \bullet \mathcal{S}^{EQ} \bullet \mathcal{P}^{EQ}\,. \tag{75}$$

$\mathcal{S}^{EQ}$ gives the shear wave velocity :

$$\mathcal{S}^{EQ} = \gamma_{22}\,N\,\mathcal{X} - \left(\gamma_{11}\,\gamma_{22} - \gamma_{12}^2\right)\omega^2\,, \tag{76}$$

which leads to an identical formula than for the SH wave (Equ. (65)-(66)).

$\mathcal{P}^{EQ}$ gives the compressional waves velocities:

$$\mathcal{P}^{EQ} = \left(P\,\tilde{R} - Q^2\right)\mathcal{X}^2 - \left(P\,\gamma_{22} + \tilde{R}\,\gamma_{11} - 2Q\gamma_{12}^2\right)\omega^2\,\mathcal{X} + \left(\gamma_{11}\,\gamma_{22} - \gamma_{12}^2\right)\omega^4\,. \tag{77}$$

The compressional and shear waves are thus decoupled. Both compressional waves correspond to singular motions of the fluid-solid system. The coupling coefficients of the potentials in each phase (Equ. (67)) are then, following the derivation used for the transversely isotropic case:

-for both compressional waves P_i:

$$\mathcal{Y}_1^{Pi} = \mathcal{Y}_3^{Pi} = 0 \,, \tag{78.a}$$

$$\mathcal{Y}_2^{Pi} = -\frac{P\,\mathcal{X} - \omega^2\,\gamma_{11}}{Q\,\mathcal{X} - \omega^2\,\gamma_{12}} \,; \tag{78.b}$$

-and for the shear wave:

$$\mathcal{Y}_1^{SV} = \mathcal{Y}_2^{SV} = 0 \,, \tag{79.a}$$

$$\mathcal{Y}_3^{SV} = -\frac{\gamma_{12}}{\gamma_{22}} = \chi^H = \chi \,. \tag{79.b}$$

It is straightforward to show the equivalence with the results obtained directly from the complete isotropic calculations (e.g., Schmitt, 1986a), i.e., $\mathcal{Y}_2^{Pi} - \xi_i = 0$ where

$$\xi_i = -\frac{1}{cp_i^2}\frac{P\tilde{R} - Q^2}{Q\gamma_{22} - \tilde{R}\gamma_{12}} + \frac{\tilde{R}\gamma_{11} - Q\gamma_{12}}{Q\gamma_{22} - \tilde{R}\gamma_{12}} \,. \tag{80}$$

Elastic Formation

For a transversely isotropic elastic formation, the porosity is equal to zero. The radial wavenumbers equation is thus obtained by considering only the first two rows and columns of the matrix $\underline{\underline{\tilde{Z}}}$ (Equ. (67)), after setting the γ_{11} terms to ρ, both the γ_{12} and γ_{22} terms to zero, and the $\underline{\underline{d}}$ tensor to the $\underline{\underline{c}}$ tensor. Taking the determinant, one obtains the usual second degree equation in q^2 (e.g., White, 1983):

$$\begin{aligned} & c_{11}\,c_{44}\,q^4 + q^2\left\{(c_{11}+c_{44})\,\rho\omega^2 - (c_{11}\,c_{33} - c_{13}^2 - 2c_{13}\,c_{44})\,k^2\right\} \\ + \quad & (\rho\omega^2 - k^2\,c_{33})\,(\rho\omega^2 - k^2 c_{44}) \qquad\qquad = 0 \,. \end{aligned} \tag{81}$$

The two roots correspond to the quasi P-wave and the quasi SV wave. Because these two waves are coupled, the solutions of the displacement potentials are:

-for the quasi P wave:

$$\begin{aligned} \Phi^{(n)P} &= \tilde{A}^{(n)}\, F(kp_t,\, k,\, \omega)\,, \\ \Gamma^{(n)P} &= \mathcal{Y}_1^P \Phi^{(n)P}\,; \end{aligned} \tag{82}$$

-and for the quasi SV wave:

$$\begin{aligned} \Phi^{(n)SV} &= \mathcal{Y}_1^{SV}\, \Gamma^{(n)SV}\,, \\ \Gamma^{(n)SV} &= \tilde{E}^{(n)}\, F(ks_V,\, k,\, \omega)\,; \end{aligned} \tag{83}$$

with

$$\mathcal{Y}_1^P = -\frac{\zeta_{11}^E(kp)}{\zeta_{12}^E(kp)}\,, \quad \text{and} \quad \mathcal{Y}_1^{SV} = -\frac{\zeta_{12}^E(ks_V)}{\zeta_{11}^E(ks_V)}\,. \tag{84}$$

where the superscript ^{E} stands for "Elastic" (i.e., $\tilde{\varphi} = 0$).

Expanding the above formulae, one finds those given by Tongtaow (1982).

The complete solution is then:

$$\begin{aligned} \Phi^{(n)} &= \Phi^{(n)P} + \Phi^{(n)SV} = \Phi^{(n)P} + \mathcal{Y}_1^{SV}\, \Gamma^{(n)SV}\,, \\ \Gamma^{(n)} &= \Gamma^{(n)P} + \Gamma^{(n)SV} = \mathcal{Y}_1^P\, \Phi^{(n)P} + \Gamma^{(n)SV}\,. \end{aligned} \tag{85}$$

The SH wavenumber is given by the equation (66) (after having performed the same modifications than previously), i.e.,

$$q^2 = ks_H^2 = \frac{c_{44}\, k^2 - \omega^2 \rho}{c_{66}}\,. \tag{86}$$

When the elastic formation is isotropic, the P and S waves are decoupled and the corresponding wavenumbers are

$$\begin{aligned} q^2 = kp^2 &= k^2 - \omega^2 / cp^2\,, \\ q^2 = ks^2 &= k^2 - \omega^2 / cs^2\,, \end{aligned} \tag{87}$$

where $cp^2 = \dfrac{\lambda_b + 2\mu_b}{\rho}$ and $cs^2 = \dfrac{\mu_b}{\rho}$. Of course, $\mathcal{Y}_1^P = \mathcal{Y}_1^{SV} = 0$.

(QUASI) BODY WAVE PROPERTIES

In this section, the properties of the (quasi) body wave phase velocities and attenuations (in the sense of Q^{-1}) are studied as a function of the only transversely isotropic permeability, the anisotropy of the skeleton, and the (anisotropic) mass coupling coefficient (i.e., tortuosity). We first present some general analytical results followed by an analysis along the principal directions in both the low and high frequency ranges. Numerical examples then allow more quantification for propagation along any direction and in the intermediate frequency range. Although the saturant fluid mobility (i.e., the permeability to the saturant fluid viscosity ratio) is the key factor, only the permeability can be anisotropic. We then refer to this last parameter.

General Analytical Formulae

The phase velocities c of the plane waves traveling in the (r, z) plane (or (x,z) plane) making an angle ψ with the z axis are obtained from the wavenumber equations by setting

$$q = i\omega \sin\psi/c \,, \tag{88.a}$$

and

$$k = \omega \cos\psi/c \,. \tag{88.b}$$

Simple algebraic manipulations yield for the SH wave (from equation (66)):

$$c_{SH} = \left\{ \left(d_{44} \cos^2\psi + d_{66} \sin^2\psi \right) / \left(\gamma_{11}^H - \gamma_{12}^{H^2} / \gamma_{22}^H \right) \right\}^{1/2} \,, \tag{89}$$

and for the quasi P_1, P_2, and SV waves (from equations (68) with $X = P_1$, P_2 and SV)

$$\begin{aligned} c_X^6\, \Xi_7 \quad & + c_X^4 \left\{ -\Xi_4 \sin^2\psi + \Xi_8 \cos^2\psi \right\} \\ & + c_X^2 \left\{ \Xi_2 \sin^4\psi - \Xi_6 \sin^2\psi \cos^2\psi + \Xi_9 \cos^4\psi \right\} \\ & - \Xi_1 \sin^6\psi + \Xi_3 \sin^4\psi \cos^2\psi - \Xi_8 \sin^2\psi \cos^4\psi + \Xi_{10} \cos^6\psi = 0 \,. \end{aligned} \tag{90}$$

The (quasi) body waves are inhomogeneous in the sense that the assciated propagation vector ($\mathcal{U}$) is complex (e.g., Borcherdt, 1973). The directions of propagation and of attenuation ("damping") are neither perpendicular (case of the pure elastic waves for which $Q^{-1} = 0$) nor parallel (case of the diffusive waves for which $Q^{-1} = 2$): the planes of constant phase and constant amplitude do not coincide. The particle motion is also affected by the only attenuation: it is elliptical. Within an isotropic formation, the

large and small axes are, respectively, $Re(\underline{\mathcal{U}})$ and $Im(\underline{\mathcal{U}})$ for the compressional waves, and perpendicular to $Im(\underline{\mathcal{U}})$ and $Re(\underline{\mathcal{U}})$ for the shear wave.

Simple formulae can be easily deduced for $\psi = 0^o$ and $\psi = 90^o$.

Vertical propagation

For vertical propagation (i.e., $\psi = 0^o$), the shear waves velocities are given by:

$$c_{SHv} = c_{SVv} = \left\{ d_{44} / \left(\gamma_{11}^H - \gamma_{12}^{H^2} / \gamma_{22}^H \right) \right\}^{1/2} . \tag{91.a}$$

These formulae are similar to those of the elastic case (e.g., White, 1983; Levin, 1979):

$$c_{SHv} = c_{SVv} = \{ c_{44} / \rho \}^{1/2} , \tag{91.b}$$

where the density is replaced by the γ_{ij} coefficients which depend on the *only horizontal permeability and mass coupling coefficients.* Such a behavior is related to the combination of the direction of propagation and the polarization of the waves as sketched in Figure 1a (at the first order, neglecting the attenuation effects).

The phase velocities of the P_{Xv} waves (X=1, 2) are solutions of a biquadratic equation:

$$c_{PX}^4 \left(\gamma_{11}^V \gamma_{22}^V - \gamma_{12}^{V^2} \right) - c_{PXv}^2 \left(d_{33} \gamma_{22}^V + \tilde{\mathcal{R}} \gamma_{11}^V - 2 Q_3 \gamma_{12}^V \right) + d_{33} \tilde{\mathcal{R}} - Q_3^2 = 0 . \tag{92.a}$$

The structure of this last is analogous to that in the complete isotropic case (see Equ. (77)). Mainly the *vertical* parameters (stiffness constants and complex permeability) play a role because the direction of propagation and the polarization are sub-parallel (Figure 1a), similarly to the elastic case where:

$$c_{Pv} = \{ c_{33} / \rho \}^{1/2} . \tag{92.b}$$

Horizontal propagation

For $\psi = 90°$, the shear waves phase velocities are:

$$c_{SHh} = \left\{ d_{66} / \left(\gamma_{11}^H - \gamma_{12}^{H^2} / \gamma_{22}^H \right) \right\}^{1/2} , \tag{93.a}$$

and

$$c_{SVh} = \left\{ d_{44} / \left(\gamma_{11}^V - \gamma_{12}^{V^2} / \gamma_{22}^V \right) \right\}^{1/2} , \tag{93.b}$$

where the "distribution" of the horizontal and vertical permeability effects is again easily understood when looking at the direction of propagation versus the direction of

polarization of the waves (Figure 1b, at the first order). The stiffnesses "repartition" follows that of the elastic case for which:

$$c_{SHh} = \{c_{66}/\rho\}^{1/2} \ , \tag{93.c}$$

and

$$c_{SVh} = \{c_{44}/\rho\}^{1/2} \ . \tag{93.d}$$

The phase velocities of the P_{Xv} waves (X =1, 2) are now solutions of a biquadratic equation where mainly the horizontal coefficients play a role:

$$c_{PX}^4 \left(\gamma_{11}^H \gamma_{22}^H - \gamma_{12}^{H^2}\right) - c_{PXv}^2 \left(d_{11}\,\gamma_{22}^H + \tilde{\mathcal{R}}\,\gamma_{11}^H - 2\,Q_1\,\gamma_{12}^H\right) + d_{11}\,\tilde{\mathcal{R}} - Q_1^2 = 0 \ , \tag{94.a}$$

as expected from the formula relative to the elastic case, i.e.,

$$c_{Ph} = \{c_{11}/\rho\}^{1/2} \ , \tag{94.b}$$

and from the direction of propagation versus the direction of polarization (Figure 1b, at the first order).

The couples of equations ((91.a); (93.b)), and ((92.a); (94.a)), show that the velocity and/or attenuation of, respectively, the SV and both compressional waves can be different in the horizontal and vertical directions, due to the only transverse isotropy of the complex permeability tensor.

Frequency Analysis Along the Principal Directions

Because of the form of the formulae for propagation along the principal directions, simple results can be derived in the low and high frequency ranges using the developments of Boutin (1987) and Schmitt (1985). For the SH-wave, no distinction of direction of propagation is necessary as it only excites the horizontal permeability. Explicit expressions being given for both the phase velocity and the attenuation (Q^{-1}), it is straightforward to deduce the form of the attenuation coefficient, i.e.,

$$\delta_j = \omega\, Q_j^{-1}/(2c_j) \ , \ j = P_1,\ P_2,\ SV,\ SH \ . \tag{95}$$

As already mentioned, the energy dissipation is due to the fluid flow related to the relative motion between the solid and liquid phases which are coupled through inertial and viscous forces. When the formation is completely isotropic, these forces are of the same order of magnitude at a so called critical frequency which is inversely proportional to the permeability of the material (more precisely, to the saturant fluid mobility). Below this frequency, i.e., in the low frequency range, the viscous forces are predominant and the (laminar) flow follows Poiseuille's law. When the inertial forces

are no longer negligible, a given repartition function of the stress in the fluid occurs (the flow is no longer uniform). In the high frequency range, the viscosity effects take place in only a very thin layer close to the pore wall. For the fast compressional wave and the shear wave, the dissipation of energy, in the sense of the inverse of the quality factor, is maximum around the critical frequency. With a transversely isotropic permeability, such a frequency can only be defined along each principal direction (e.g., equ. (35)):

$$f_{c_l} = \frac{\eta \tilde{\varphi}^2}{2\pi \tilde{k}_l \rho_{22_l}(0)} ,$$

where the subscript l denotes the horizontal plane (l=h) or the vertical direction (l=v). The low (high) frequency range of a transversely isotropic formation can only be defined with respect to the lowest (highest) "principal" critical frequency.

In order to have a synthetic notation, the subscript l denoting the principal direction will be implicitly equal to 1 or 3 for both compressional waves, and to 6 or 4 for the (quasi) shear waves, when referring to the horizontal plane of the vertical direction, respectively. $l\perp$ will denote the principal direction perpendicular to l. Finally, we will write

$$\rho = (1 - \tilde{\varphi})\rho_s + \tilde{\varphi}\rho_f . \tag{96}$$

Low frequency range

When the frequeny tends to zero, the viscous coupling coefficients verify Darcy's law, i.e.,

$$\lim_{\omega \to 0} b_l(\omega) = \eta \, \tilde{\varphi}^2 / \tilde{k}_l , \tag{97}$$

while the mass coupling coefficients $\rho_{22_l}(\omega)$ tend to a constant characteristic of the pore geometry. With the cylindrical duct model, it is equal to:

$$\lim_{\omega \to 0} \rho_{22_l}(\omega) = \rho_{22_l}(0) = \frac{4}{3} \tilde{\tau}_l \, \tilde{\varphi} \rho_f . \tag{98}$$

Such limits are valid at the second order with respect to the frequency (i.e., $(0(\omega^2))$.

SH-wave.

$$\lim_{\omega \to 0} c^2_{SH}(\psi) = \frac{d_{44} \cos^2 \psi + d_{66} \sin^2 \psi}{\rho} , \tag{99.a}$$

$$\lim_{\omega \to 0} Q^{-1}_{SH}(\psi) = \omega \frac{\tilde{k}_h}{\eta} \frac{\rho_f^2}{\rho} . \tag{99.b}$$

Quasi SV-wave.

$$\lim_{\omega\to 0} c_{SVl}^2 = d_{ll}/\rho \,, \tag{100.a}$$

$$\lim_{\omega\to 0} Q_{SVl}^{-1} = \omega \frac{\tilde{k}_{l\perp}}{\eta} \frac{\rho_f^2}{\rho} \,. \tag{100.b}$$

Quasi P_1-wave.

$$\lim_{\omega\to 0} c_{P1l}^2 = \frac{d_{ll} + \tilde{\mathcal{R}} + 2Q_l}{\rho} \,, \tag{101.a}$$

$$\lim_{\omega\to 0} Q_{P1l}^{-1} = \omega \frac{\tilde{k}_l}{\eta} \frac{\rho_f^2}{\rho} \left(1 + \frac{\rho}{\rho_f} \frac{Q_l + \tilde{\mathcal{R}}}{\tilde{\varphi}(d_{ll} + \tilde{\mathcal{R}} + 2Q_l)}\right)^2 \,. \tag{101.b}$$

These limits indicate that the velocities of the SH-wave, the quasi SV-wave and the quasi P_1-wave correspond to those of an elastic medium whose density is ρ and whose characteristics are independent from the permeability (saturant fluid mobility). The (quasi) body waves are however attenuated proportionally to a "directional" permeability. Their attenuation (Q^{-1}) and attenuation coefficient δ_j are also proportional to ω and ω^2, respectively.

Quasi P_2-wave.

$$\lim_{\omega\to 0} c_{P2l}^2 = 2\omega \frac{\tilde{k}_l}{\eta\tilde{\varphi}^2} \frac{d_{ll}\tilde{\mathcal{R}} - Q_l^2}{d_{ll} + \tilde{\mathcal{R}} + 2Q_l} \,, \tag{102.a}$$

$$\lim_{\omega\to 0} Q_{P2l}^{-1} = 2 \,. \tag{102.b}$$

The quasi compressional wave of the second kind is a diffusive wave whose phase velocity tends to zero proportionally to the frequency. Contrary to the quasi P_1-wave, to the quasi SV-wave and to the SH-wave, its phase velocity increases and its attenuation coefficient decreases with increasing "directional" permeability. It corresponds to an out of phase motion between the solid and liquid phases.

High frequency range

When the frequency tends to infinity, the complex spectral signature along each principal direction is:

$$\lim_{\omega\to\infty} H_l(\omega) = i\omega \frac{\tilde{\tau}_l}{\tilde{\varphi}} \rho_f \left\{1 + (1-i)\sqrt{\frac{\tilde{k}_l\,\tilde{\tau}_l\,\rho_f}{2\eta\,\tilde{\varphi}\,\omega}} + 0(\omega^{-1})\right\} \,, \tag{103}$$

so that

$$\lim_{\omega\to\infty} b_l(\omega) \propto \omega^{1/2} , \tag{104.a}$$

and,

$$\lim_{\omega\to\infty} \rho_{22_l}(\omega) = \rho_{22_l}(\infty) = \tilde{\eta}_l\, \tilde{\varphi}\rho_f . \tag{104.b}$$

One then obtains,

SH-**wave.**

$$\lim_{\omega\to\infty} c^2_{SH}(\psi) = \frac{d_{44}\cos^2\psi + d_{66}\sin^2\psi}{(1-\tilde{\varphi})\rho_s + \tilde{\varphi}\rho_f(1-1/\tilde{\tau}_h)} , \tag{105.a}$$

$$\lim_{\omega\to\infty} \mathcal{Q}^{-1}_{SH}(\psi) = \sqrt{\frac{\eta\tilde{\varphi}\tilde{\tau}_h}{2\omega\tilde{k}_h\rho_f}}\,\frac{1}{(\rho\,\tilde{\tau}_h/\tilde{\varphi}\rho_f)-1} . \tag{105.b}$$

Quasi *SV*-**wave.**

$$\lim_{\omega\to\infty} c^2_{SVl} = \frac{d_{ll}}{(1-\tilde{\varphi})\rho_s + \tilde{\varphi}\rho_f(1-1/\tilde{\tau}_{l\perp})} , \tag{106.a}$$

$$\lim_{\omega\to\infty} \mathcal{Q}^{-1}_{SVl} = \sqrt{\frac{\eta\tilde{\varphi}\tilde{\tau}_{l\perp}}{2\omega\tilde{k}_{l\perp}\rho_f}}\,\frac{1}{(\rho\tilde{\tau}_{l\perp}/\tilde{\varphi}\rho_f)-1} . \tag{106.b}$$

Both shear wave velocities are stabilized, reaching a constant value. It has to be noted that with a unit tortuosity along the appropriate principal direction, they tend toward the velocity of the dry rock, the fluid being motionless.

Quasi compressional waves. The phase velocities of the quasi compressional waves are solution of biquadratic equations where the complex coupling coefficients γ^L_{ij} are replace by the real high frequency limit of the mass coupling coefficients $\rho_{ij_l}(\infty)$ (hereafter noted ρ_{ij_l} for clarity), i.e.,

$$c^4_{PXl}(\infty)(\rho_{11_l}\rho_{22_l}-\rho^2_{12_l}) - c^2_{PXl}(\infty)(d_{ll}\rho_{22_l} + \tilde{\mathcal{R}}\rho_{11_l} - 2Q_l\rho_{12_l}) + d_{ll}\tilde{\mathcal{R}} - Q_l^2 = 0 , \tag{107.a}$$

where X=1, 2. The phase velocity of the quasi compressional wave of the second kind, again associated with an out of phase motion between the two phases, never exceeds that of the saturant fluid.

The associated attenuation is:

$$\lim_{\omega\to\infty} \mathcal{Q}^{-1}_{PXl} = \frac{1}{2}\sqrt{\frac{\eta\tilde{\tau}_l\rho_f}{2\omega\tilde{k}_l\tilde{\varphi}}}\,\tilde{\tau}_l\left[\frac{\alpha_l^2}{c_{ll}} + \beta\right] \mathcal{M}(c_{PXl}(\infty) , \tag{107.b}$$

with

$$\mathcal{M}(c_{PXl}(\infty)) = c^2_{PXl}(\infty) \cdot \frac{c^2_{PXl}(\infty) \cdot \dfrac{\rho}{c_{ll} + \alpha_l^2/\beta} - 1}{c^2_{PXl}(\infty) \cdot \dfrac{\rho + \rho_f \left[\beta(c_{ll} + \alpha_l^2/\beta)\tilde{\tau}_l/\tilde{\varphi} - 2\alpha_l\right]}{2c_{ll}} - 1},$$

where α_l, and β are respectively given by the equations (37) and (38), while c_{ll} indicates the stiffness constant of the skeleton.

All four body waves tend to an elastic mode as their attenuations ($\mathcal{Q}^{-1}$), inversely proportional to a "directional" permeability, go to zero proportionally to $\omega^{-1/2}$. However, they are all affected by an attenuation coefficient which is proportional to the square root of the frequency.

Numerical Examples

Numerical calculations allow a quantification of the "directional" permeability notion as well as of the (quasi) body waves behavior in the intermediate frequency range. Table 1 gives the parameter of the formations considered. No anelatic attenuation is introduced in the skeleton. Unless specified otherwise, the tortuosity is equal to unity in both the horizontal plane and the vertical direction, the pore shape being the cylindrical duct model. For a given angle of propagation with respect to the vertical, the calculations are performed in the frequency range [1, 10^7] Hz.

Transversely isotropic permeability only

The effects of the only transversely isotropic permeability are first investigated. The saturated porous formation is a 15% sandstone (Table 1) whose horizontal and vertical permeability are respectively equal to 1 darcy and 100 mdarcies. The associated critical frequencies are equal to 18.142 kHz and 181.42 kHz, respectively.

Figure 2 shows the phase velocity and the attenuation of the quasi P_1-wave (a), the quasi P_2-wave (b), the quasi SV wave (c) and the SH wave (d) as a function of the frequency. For each wave, the different curves correspond to values of the angle of propagation with respect to the vertical which varies from 0^o to 90^o by step of 15^o. Also displayed are the results obtained with a 1 darcy and a 100 mdarcies isotropic permeability. For both quasi compressional waves, they are superimposed to the curves obtained with a horizontal and vertical direction of propagations, respectively. The correspondance is reverse for the quasi SV wave. The SH-wave is affected by the only horizontal permeability. With an isotropic skeleton, its characteristics are thus

equal to those obtained with the 1 darcy isotropic permeability, whatever the angle of propagation.

In both the low and high frequency ranges (i.e., $f < f_{c_h}$ and $f > f_{c_v}$), the quasi body wave phase velocities are independent of the angle of propagation because of the isotropy of the skeleton. They follow the equations previously derived, using isotropic stiffness constants. Only their attenuations vary. Neglecting the coupling effects, the variations can be explained by the notion of directional permeability defined as:

$$\tilde{k}(\psi,\, P_i) = \tilde{k}_v \cos^2 \psi + \tilde{k}_h \sin^2 \psi \;, \tag{108}$$

and

$$\tilde{k}(\psi,\, SV) = \tilde{k}_h \cos^2 \psi + \tilde{k}_v \sin^2 \psi \;. \tag{109}$$

The 90^o rotation between the two above formuale, which are analogous to the first definition of the directional permeability by Bear (1967), is related to the polarization of each wave.

With a complete isotropic formation permeability, the intermediate frequency range (i.e., $f \simeq f_c$),is characterized by the occurence of the body wave velocities dispersion. The P_1 and S waves also reach their maximum of attenuation. A permeability decrease (resp. increase) has no effect upon the absolute value of the body wave velocities and maxima of attenuation. The shift toward higher (resp. lower) frequency of the critical frequency only results in an equal shift of the dispersion and attenuation curves (see Figure 2d).

With a transversely isotropic permeability, such a behavior hold true only for propagation along the principal directions (Figures 2a, 2b, and 2c). Because of the frequency dependence of the inertial and viscous forces and of the coupling phenomena, the notion of directional permeability is not sufficient to explain the variations in the phase velocity slopes and in the attenuations of the quasi body waves. For intermediate values of the angle of propagation, the quasi P_1-wave and quasi SV-wave attenuations reach maxima more or less well located in frequency and smaller than those relative to the principal directions (the tortuosity tensor being isotropic).

The analysis as a function of the frequency has been motivated by the biphase character of the material. For transversely isotropic elastic formations, the quasi body wave velocities are presented as a function of the angle of propagation. Figures 3a to 3d show the (quasi) body wave phase velocities and attenuations in that way for different frequencies varying from 10^2 Hz to 10^7 Hz. The velocity anisotropy of the quasi P_1-wave and of the quasi SV-wave introduced by the only permeability is seen to be rather small, more pronounced in the intermediate frequency range. The attenuation anisotropy is more important. In absolute value, the quasi P_1-wave attenuation is small and will be superseded by any anelastic attenuation. This is not the case for both shear waves, especially in the intermediate frequency range. The quasi slow P_2 wave, characteristics

of a saturated porous material, is much more affected. Interverting the horizontal and vertical permeabilities, the variations of all three quasi body waves characteristics will be symmetrical with respect to the 45° propagation angle for each frequency.

Transversely isotropic formation

Supplementary "mechanical" anisotropy is introduced into the fast sandstone by increasing the horizontal P-wave velocity of the skeleton by $\simeq$ 5%and the horizontal SH-wave velocity of the skeleton by $\simeq$ 12% (Table 1). All others parameters have been kept constant, so that the critical frequencies are not modified. Table 2 gives the low and high frequency limits of the phase velocities along both principal directions.

As a function of the angle of propagation with respect to the vertical, the variations of the (quasi) body wave phase velocities (Figures 4a to 4d) are now similar to those obtained with a simple transversely isotropic elastic formation (e.g., Levin, 1979; Berryman, 1979). Both quasi P_1-wave and SH-wave phase velocities increase with increasing angle of propagation, while the quasi SV-wave phase velocity exhibits a maximum around 45° which may be associated with the so called "bow tie" of the group velocity (Berryman, 1979). Although small, the anisotropy of the skeleton thus supersedes that induced by the permeability (Fig. 4a, c, d) which is however still detectable through the frequency variations and the difference between the SV_h and SV_v phase velocities in the intermediate frequency range.

With completely isotropic saturated porous formations, it is known that an estimation of the slow P_2-wave velocity can be obtained, in both the low and high frequency ranges, from the elastic constants of the most compressible constituent (the inverse rule holds for the fast P_1-wave phase velocity). In the present example, the skeleton is much less compressible than the saturant fluid. The quasi slow P_2 wave phase velocity variations (Figure 4c) are then still more representative of the only transversely isotropic permeability (see Figure 3c).

The attenuations of the quasi P_1-wave, quasi SV-wave, and SH wave, representative of the two phase character of the formation, are little affected by the skeleton anisotropy. One can only noticed a slight increase in the quasi P_1-wave attenuation beyond an angle of 45°. As it is shown in Figures 5a to 5d, the directional permeability can still be used in the low and high frequency ranges. For the quasi P_1 wave, such a result is however dependent on both the degree of anisotropy and the stiffness of the skeleton. This restriction is illustrated in Figures 6a to 6d which display the (quasi) body waves velocities and attenuations computed with a less rigid and more porous formation. The degree of anisotropy of the skeleton is also more important while the complex permeability tensor is identical (see Tables 1 and 3).

Mass coupling coefficient (tortuosity) effects

Whatever the pore shape, the mass coupling coefficient decreases with increasing frequency (e.g., Schmitt, 1986a, c). Because of the chosen cylindrical duct model, an increase of the mass coupling coefficient is equivalent to an increase of the tortuosity (e.g., equ. (45)) and identical in the all frequency range. One has to keep in mind that other pore geometries may lead to more or less important frequency dependent variations (e.g., Auriault et al., 1985; Schmitt, 1986c). However, the effects of the mass coupling coefficients variations only occur when the inertial forces are no more negligible, i.e., in the high frequency range and, in a lesser extent, in the intermediate frequency range. The following study can then be considered as general.

Along each principal direction, the inertial coupling between both phases is of the form:

$$\rho_{12_l}(\omega)\,(\underline{U}-\underline{u}) = [\tilde{\varphi}\rho_f - \rho_{22_l}(\omega)]\,(\underline{U}-\underline{u})\ . \tag{110}$$

Increasing the mass coupling coefficients $\rho_{22_l}(\omega)$ thus decreases the relative displacement between the liquid and solid phases: the formation is less biphase. As a result, the high frequency limits of the (quasi) body wave phase velocities and attenuations decrease (see equ. (105) to (107)). The low frequency values remain unchanged (see equ. (99) to (102)) so that the dispersions also decreases. Last, the critical frequency decreases (e.g., equ. (35)).

Figure 7 shows the results obtained with the fast transversely isotropic sandstone and tortuosity values equal to three along both principal directions. Compare to Figure 4, and similarly to a complete isotropic situation, the dispersion decrease is seen to be more important for the quasi slow P_2-wave velocity (see also Table 2), proportional to a function of $1/\tilde{\tau}_l$ (e.g., Johnson et al., 1982). The overall shape of the attenuation curves, as well as the low frequency values, remain unchanged whatever the angle of propagation. The maxima of attenuation of the quasi P_1-wave and the quasi SV-wave are decreased, associated with lower frequencies.

As well as the permeability, the mass coupling coefficient can be anisotropic. Figure 8 displays the results as a function of the frequency when the horizontal and vertical tortuosities are respectively equal to 1 and 3. The high frequency limit of the quasi slow P_2-wave velocity now varies as a function of a directional high frequency mass coupling coefficient which can be defined as the directional permeability (equ. (108)). Such variations hold with the softer formation (see Table 3). The attenuation curves of all three body waves are also affected. The maxima of attenuation of the quasi P_1 wave (and the quasi SV wave) continuously decrease (resp. decrease) with increasing angle of propagation, and are more well located in frequency.

The effects upon the velocities are predominant in the high frequency range, which

corresponds to the ultrasonic measurements frequency domain. As a function of the angle of propagation with respect to the vertical, Figure 9 shows the results obtained at a frequency equal to 10^7 Hz with various combinations of the horizontal and vertical tortuosities (see also Table 2). In such a high frequency range, the anisotropy of the permeability does not play any role. Only the effects associated with the stiffness tensor of the skeleton and the tortuosity tensor remain, superimposed to each others. The velocity variations of the quasi P_1 wave, the quasi SV wave and the SH wave induced by the only tortuosity do not exceed few percent but may be detectable. For instance, they emphasize the possible discrepancy between the horizontally and vertically propagating SV wave velocities (Figure 9c; see also Figure 8c). The most important variations refer to the quasi slow P_2-wave velocity (Figure 9b) which is practically unaffected by the skeleton anisotropy. Caution must then be taken when estimating the tortuosity (i.e., the high frequency mass coupling coefficient) through the slow P_2-wave velocity, even when the skeleton is isotropic. As another consequence, significant changes may occur during any high frequency reflexion-transmission experiments. Although small in absolute value, the attenuations of all four waves exhibit important relative variations.

CONCLUSIONS

The constitutive equations for a general anisotropic saturated porous formation have been presented, using the results of homogenization theory. Solution for wave propagation in a transversely isotropic saturated porous formation, where the axes of symmetry of both the skeleton and the complex permeability tensor coincide, has been derived as part of the cylindrical well logging geometry.

Four dispersive and dissipative waves propagate in a transversely isotropic saturated porous formation: two quasi compressional waves, a quasi SV wave and a SH wave. All three quasi body waves approach the isotropic P_1 wave, slow P_2 wave, and S wave only as the degree of anisotropy of both the skeleton and the permeability tensor vanishes. Along the principal directions, their complex velocities are solutions of equations similar to those of the isotropic case. The stiffness constants and the complex coupling coefficients involved refer to the same direction for the compressional waves. They refer to perpendicular directions for the SV wave. The SH wave only excites the horizontal permeability, whatever its angle of propagation with respect to the vertical.

Energy dissipation is due to the fluid flow related to the relative motion between the two phases which are coupled through friction and inertial forces. Along both principal directions, these forces are of the same order of magnitude at a critical frequency which depends on the saturant fluid properties, the porosity, and the corresponding mass coupling coefficient and permeability (similarly to the isotropic situation). Below the lowest critical frequency, i.e., in the low frequency range, the viscous forces are

predominant and the (laminar) fluid flow follows Poiseuille law. Transverse isotropy of the only permeability leads to anisotropy of the quasi P_1-wave and quasi SV-wave attenuations (in the sense of Q^{-1}) which increase proportionally to the frequency. The quasi P_2 wave is a diffusive wave, whatever its angle of propagation with respect to the vertical. When the inertial forces are no longer negligible, a given repartition function of the stress in the fluid occur (the flow is no longer laminar). In such an intermediate frequency range, the dissipation of energy of both the quasi P_1 wave and the quasi SV wave reaches maxima more or less well located in frequency, depending on the anisotropy of both the permeability and the mass coupling coefficient and on their angle of propagation with respect to the vertical. Above the highest critical frequency, i.e., in the high frequency range, the viscosity effects take place in only a very thin layer close to the pore wall. The attenuation of all three quasi body waves is then proportional to the inverse of the square root of the frequency. Its anisotropy is function of that of both the permeability and the mass coupling coefficient. The attenuation of the SH wave behaves like in an isotropic formation, with respect to the horizontal properties of the complex permeability tensor.

Whatever the frequency, the quasi P_1-wave, quasi SV-wave and SH-wave velocities are primarily governed by the anisotropy of the skeleton. The anisotropy of the only permeability has very little effects, located in the intermediate frequency range. In the high frequency range, an anisotropy of the mass coupling coefficient leads to slightly different quasi SV-wave velocities along the principal directions, contrary to the pure elastic situation. At the opposite, the slow P_2-wave velocity is mostly representative of the transeverse isotropy of the permeability in the intermediate frequency range and of that of the mass coupling coefficient in the high frequency range.

The degree of anisotropy of the attenuation induced by the two phase character of the formation is greater than that of the velocity (due to the skeleton). Such a property may be of useful practical interest, even if it refers to the superimposed anelasticity of the skeleton which may be dominant, especially in the low frequency range.

ACKNOWLEDGEMENTS

This work was supported by the Full Waveform Acoustic Logging Consortium at M.I.T.

REFERENCES

Achenbach, J.D., *Wave propagation in elastic solids*; North-Holland, 1973.

Auld, B.A., *Acoustic fields and waves in solids*; John Wiley & Sons, 1973.

Auriault, J.L., 1980, Dynamic behavior of a porous medium saturated by a newtonian fluid *Int. J. Eng. Sci., 18*, 775–785, 1980.

Auriault, J.L., Homogenization. Application to porous saturated media. Wladyslawowo Summer School, 1983.

Auriault, J.L., *Mécanique des milieux poreux saturés déformables*; Institut de Mécanique de Grenoble, France, 1986.

Auriault, J. L., Borne, L., and Chambon, R., Dynamics of porous saturated media, checking of the generalized law of Darcy; *J. Acoust. Soc. Am., 77*, 1641–1650, 1985.

Backus, G.E., Long wave elastic anisotropy produced by horizontal layering; *J. Geophys. Res., 67*, 4427–4440, 1962.

Badiey, M., and Yamamoto, T., Propagation of acoustic normal modes in a homogeneous ocean overlaying layered anisotropic porous beds; *J. Acoust. Soc. Am., 77*, 954–961, 1985.

Bear, J., *Dynamics of fluids in porous media*; American Elsevier, 1967.

Berryman, J.G., Long-wave elastic anisotropy in transversely isotropic media; *Geophysics, 44*, 896–917, 1979.

Berryman, J.G., and Thigpen, L., Linear dynamic poroelasticity with microstructure for partially saturated solids; *J. Appl. Mech., 52*, 345–350, 1985.

Biot, M.A., Theory of elasticity and consolidation for a porous anisotropic solid; *J. Appl. Phys., 26*, 182–185, 1955.

Biot, M. A., Theory of propagation of elastic waves in a fluid saturated porous rock. I. Low frequency range; *J. Acoust. Soc. Am., 28*, 168–178, 1956a.

Biot, M. A., Theory of propagation of elastic waves in a fluid saturated porous rock. II. Higher frequency range; *J. Acoust. Soc. Am., 28*, 179–191, 1956b.

Biot, M.A., Mechanics of deformation and acoustic propagation in porous media; *J. Appl. Phys., 33*, 1482–1488, 1962a.

Biot, M.A., Generalized theory of acoustic propagation in porous dissipative media; *J.*

Acoust. Soc. Am., 34, 1254–1264, 1962b.

Borcherdt, R.D., Energy and plane waves in linear viscoelastic media, *J. Geophys. Res., 78*, 2442–2453, 1973.

Borne, L.,*Contribution à l'étude du comportement dynamique des milieux poreux saturés déformables. Etude de la loi de filtration dynamique*, Thèse de Docteur Ingénieur, Univ. of Grenoble, France, 1983.

Boutin, C.,*Dynamique des milieux poreux déformables. Fonctions de Green. Perméamètre dynamique*, Ph.D. thesis, Univ. of Grenoble, France, 1987.

Boutin, C., Bonnet, B., and Bard, P.Y., Green's function and associated sources in infinite and stratified poroelastic media; Geophys. J. R. Astr. Soc., in press, 1987.

Brown, R.J.S., and Korringa, J, On the dependence of the elastic properties of a porous rock on the compressibility of the pore fluid; *Geophysics, 40*, 608–616, 1975.

Johnson, D.L., and Plona, T.J., Acoustic slow waves and the consolidation transition; *J. Acoust. Soc. Am., 72*, 556–565, 1982.

Johnson, D.L., Plona, T.J., Scala, C., Pasierb, F., and Kojima, F., Tortuosity and acoustic slow waves; *Phys. Rev. Lett., 49*, 1840–1844, 1982.

Levin, F.K., Seismic velocities in transversely isotropic media; *Geophysics, 44*, 918–936, 1979.

Plona, T.J., and Johnson, D.L., Experimental study of the two bulk compressional modes in water saturated porous structures; *Ultrasonic Symposium,* 864–872, 1980.

Schmitt, D.P.,*Simulation numérique de diagraphies acoustiques. Propagation d'ondes dans des formations cylindriques axisymétriques radialement stratifiées incluant des milieux élastiques et/ou poreux saturés.* Ph.D. thesis. Grenoble Univ., France, 1985.

Schmitt, D.P., Full wave synthetic acoustic logs in saturated porous media. Part I. A review of Biot's theory.*Full Waveform Acoustic Logging Consortium Ann. Rep.,* 105–175, MIT, Cambridge, 1986a.

Schmitt, D.P., Full wave synthetic acoustic logs in saturated porous media. Part III. Pore shape and pore geometry effects. *Full Waveform Acoustic Logging Consortium Ann. Rep.,* 281–330, MIT, Cambridge, 1986b.

Schmitt, D.P., and Cheng, C.H., Shear wave logging in (multilayered) elastic formations: an overview; *Full Waveform Acoustic Logging Consortium Ann. Rep.,* 213–268, MIT, Cambridge, 1987.

Schoenberg, M., Reflection of elastic waves from periodically stratified media with

interfacial slip; *Geophys. Prosp., 31,* 265–292, 1983.

Tongtaow, C., *Wave propagation along a cylindrical borehole in transversely isotropic formation*; Ph.D. thesis, Colorado School of Mines, Golden, Colorado, 1982.

White, J.E., *Underground Sound*; Elsevier, Holland, 1983.

Yew, C.H., and Weng, X., A study of reflection and refraction of waves at the interface of water and porous sea ice; *J. Acoust. Soc. Am., 82,* 342–353, 1987.

Parameter	"Fast" sandstone	Slow formation
K_s (10^{10} Pa)	3.79	3.5
ρ_s (kg/m^3)	2650	2600
c_f (m/s)	1500	1500
ρ_f (kg/m^3)	1000	1000
η (Pa·s)	10^{-3}	10^{-3}
c_{11} (10^{10} Pa)	3.33725667	0.9568
c_{13} (10^{10} Pa)	0.91251037	0.23296
c_{33} (10^{10} Pa)	3.0338697	0.832
c_{44} (10^{10} Pa)	1.0606797	0.29952
c_{66} (10^{10} Pa)	1.32258497	0.419328
$\tilde{\varphi}$ (%)	15	20
$\tilde{k}_h$ (darcy)	1.	1.
$\tilde{k}_v$ (darcy)	0.1	0.1

Table 1. Formations parameters.

Direction of propgation	Frequency	Tortuosity	c_{P1} (m/s)	c_{P2} (m/s)	c_{SV} (m/s)	c_{SH} (m/s)
Vertical	0	No effect	3792.7	0	2101.2	2101.2
Horizontal	0	No effect	3950.5	0	2101.2	2349.2
Horizontal	∞	1	4108.8	1301.6	2170.0	2426.1
	∞	2	4093.6	923.8	2134.7	2386.7
	∞	3	4088.9	755.1	2123.4	2374.0
Vertical	∞	1	3950.0	1292.5	2170.0	2170.0
	∞	2	3932.6	918.0	2134.7	2134.7
	∞	3	3927.2	750.5	2123.4	2123.4

Table 2. Phase velocities of the (quasi) body waves relative to the transversely isotropic "fast" sandstone. The tortuosity is assumed to be isotropic.

Direction of propgation	Frequency	Tortuosity	c_{P1} (m/s)	c_{P2} (m/s)	c_{SV} (m/s)	c_{SH} (m/s)
Vertical	0	No effect	2600.5	0	1146.2	1146.2
Horizontal	0	No effect	2702.4	0	1146.2	1356.2
Vertical	∞	1	2894.0	940.1	1200.0	1200.0
	∞	2	2804.0	686.0	1172.2	1172.2
	∞	3	2776.0	565.8	1163.3	1163.3
Horizontal	∞	1	2983.0	977.5	1200.0	1419.9
	∞	2	2902.6	710.4	1172.2	1386.9
	∞	3	2877.4	585.1	1163.3	1376.4

Table 3. Phase velocities of the (quasi) body waves relative to the transversely isotropic slow formation. The tortuosity is assumed to be isotropic.

APPENDIX

Algebraic details

Expanding the divergence stress operator in the cylindrical coordinates system, the equations of motion (22) and (24), with respect to a nth order multipole source, are, for a transversely isotropic saturated porous material:

$$\begin{aligned}
\sigma_{rr}^{(n)},_r + \frac{1}{r}\sigma_{rr}^{(n)} - \frac{1}{r}\sigma_{\theta\theta}^{(n)} + \sigma_{rz}^{(n)},_z + \frac{1}{r}\sigma_{r\theta}^{(n)},_\theta &= -\omega^2\,\gamma_{11}^H\,u^{(n)} - \omega^2\,\gamma_{12}^H\,U^{(n)}\,,\\
\frac{1}{r}\sigma_{\theta\theta}^{(n)},_\theta + \sigma_{\theta z}^{(n)},_z + \sigma_{r\theta}^{(n)},_r + \frac{2}{r}\sigma_{r\theta}^{(n)} &= -\omega^2\,\gamma_{11}^H\,v^{(n)} - \omega^2\,\gamma_{12}^H\,V^{(n)}\,,\\
\sigma_{zz}^{(n)},_z + \frac{1}{r}\sigma_{\theta z}^{(n)},_\theta + \frac{1}{r}\sigma_{rz}^{(n)} + \sigma_{rz}^{(n)},_r &= -\omega^2\,\gamma_{11}^V\,w^{(n)} - \omega^2\,\gamma_{12}^V\,W^{(n)}\,,\\
s^{(n)},_r &= -\omega^2\,\gamma_{12}^H\,u^{(n)} - \omega^2\,\gamma_{22}^H\,U^{(n)}\,,\\
\frac{1}{r}s^{(n)},_\theta &= -\omega^2\,\gamma_{12}^H\,v^{(n)} - \omega^2\,\gamma_{22}^H\,V^{(n)}\,,\\
s^{(n)},_z &= -\omega^2\,\gamma_{12}^V\,w^{(n)} - \omega^2\,\gamma_{22}^V\,W^{(n)}\,,
\end{aligned} \qquad (A-1)$$

where the superscripts H and V indicate the horizontal ($(r,\,\theta)$ plane) and vertical (z) directions.

Denoting, $\varepsilon^{(n)} = \nabla \cdot \vec{U}^{(n)}$, the stress-strain relations (Equ. (21) and (23)) can be written as:

$$\begin{aligned}
\sigma_{rr}^{(n)} &= d_{11}\left\{e_{rr}^{(n)} + e_{\theta\theta}^{(n)}\right\} - 2\,d_{66}e_{\theta\theta}^{(n)} + d_{13}\,e_{zz}^{(n)} + Q_1\,\varepsilon^{(n)}\,,\\
\sigma_{\theta\theta}^{(n)} &= d_{11}\left\{e_{rr}^{(n)} + e_{\theta\theta}^{(n)}\right\} - 2\,d_{66}e_{rr}^{(n)} + d_{13}\,e_{zz}^{(n)} + Q_1\,\varepsilon^{(n)}\,,\\
\sigma_{zz}^{(n)} &= d_{13}\left\{e_{rr}^{(n)} + e_{\theta\theta}^{(n)}\right\} + d_{33}\,e_{zz}^{(n)} + Q_3\,\varepsilon^{(n)}\\
\sigma_{\theta z}^{(n)} &= 2\,d_{44}\,e_{\theta z}^{(n)}\,,\\
\sigma_{rz}^{(n)} &= 2\,d_{44}\,e_{rz}^{(n)}\,,\\
\sigma_{r\theta}^{(n)} &= 2\,d_{66}\,e_{r\theta}^{(n)}\,,\\
s^{(n)} &= Q_1\left\{e_{rr}^{(n)} + e_{\theta\theta}^{(n)}\right\} + Q_3\,e_{zz}^{(n)} + \tilde{\mathcal{R}}\,\varepsilon^{(n)}\,.
\end{aligned} \qquad (A-2)$$

The strain-displacement relations for the solid phase are given by the usual formulae

(e.g., Achenbach, 1973):

$$\begin{aligned} e_{rr}^{(n)} &= u^{(n)}{}_{,r} \ , \\ e_{\theta\theta}^{(n)} &= \frac{1}{r}u^{(n)} + \frac{1}{r}v^{(n)}{}_{,\theta} \ , \\ e_{zz}^{(n)} &= w^{(n)}{}_{,z} \ , \\ 2\,e_{\theta z}^{(n)} &= v^{(n)}{}_{,z} + \frac{1}{r}w^{(n)}{}_{,\theta} \ , \\ 2\,e_{rz}^{(n)} &= u^{(n)}{}_{,z} + w^{(n)}{}_{,r} \ , \\ 2\,e_{r\theta}^{(n)} &= \frac{1}{r}u^{(n)}{}_{,\theta} + v^{(n)}{}_{,r} - \frac{1}{r}v^{(n)} \ . \end{aligned} \qquad (A-3)$$

Equivalent relations hold for the saturant fluid so that

$$\varepsilon^{(n)} = U^{(n)}{}_{,r} + \frac{1}{r}U^{(n)} + \frac{1}{r}V^{(n)} + W^{(n)}{}_{,z} \ . \qquad (A-4)$$

Introducing these three last sets of relations into the equations of motion (Equ. (68)), one finally obtains the following six equations:

$$\begin{aligned} & d_{11}\left(u^{(n)}{}_{,rr} + \frac{1}{r}u^{(n)}{}_{,r} - \frac{1}{r^2}u^{(n)} + \frac{1}{r}v^{(n)}{}_{,\theta r} - \frac{1}{r^2}v^{(n)}{}_{,\theta}\right) \\ + \ & d_{13}\,w^{(n)}{}_{,rz} + d_{44}\left(u^{(n)}{}_{,zz} + w^{(n)}{}_{,rz}\right) \\ + \ & d_{66}\left(\frac{1}{r^2}u^{(n)}{}_{,\theta\theta} - \frac{1}{r}v^{(n)}{}_{,\theta r} - \frac{1}{r^2}v^{(n)}{}_{,\theta}\right) \\ + \ & Q_1\left(U^{(n)}{}_{,rr} + \frac{1}{r}U^{(n)}{}_{,r} - \frac{1}{r^2}U^{(n)} + \frac{1}{r}V^{(n)}{}_{,\theta r} - \frac{1}{r^2}V^{(n)}{}_{,\theta} + W^{(n)}{}_{,rz}\right) \\ = \ & -\omega^2\,\gamma_{11}^H\,u^{(n)} - \omega^2\,\gamma_{12}^H\,U^{(n)} \ , \end{aligned} \qquad (A-5.a)$$

$$\begin{aligned} & d_{11}\left(\frac{1}{r}u^{(n)}{}_{,\theta r} + \frac{1}{r^2}u^{(n)}{}_{,\theta} + \frac{1}{r^2}v^{(n)}{}_{,\theta\theta}\right) \\ + \ & d_{13}\,\frac{1}{r}w^{(n)}{}_{,\theta z} + d_{44}\left(v^{(n)}{}_{,zz} + \frac{1}{r}w^{(n)}{}_{,\theta z}\right) \\ + \ & d_{66}\left(-\frac{1}{r}u^{(n)}{}_{,\theta r} + \frac{1}{r^2}u^{(n)}{}_{,\theta} + v^{(n)}{}_{,rr} + \frac{1}{r}v^{(n)}{}_{,r} - \frac{1}{r^2}v^{(n)}\right) \\ + \ & Q_1\left(\frac{1}{r}U^{(n)}{}_{,\theta r} + \frac{1}{r^2}U^{(n)}{}_{,\theta} + \frac{1}{r^2}V^{(n)}{}_{,\theta\theta} + \frac{1}{r}W^{(n)}{}_{,\theta z}\right) \\ = \ & -\omega^2\,\gamma_{11}^H\,v^{(n)} - \omega^2\,\gamma_{12}^H\,V^{(n)} \ , \end{aligned} \qquad (A-5.b)$$

$$\begin{aligned} & d_{33}\,w^{(n)}{}_{,zz} + d_{13}\left(u^{(n)}{}_{,rz} + \frac{1}{r}u^{(n)}{}_{,z} + \frac{1}{r}v^{(n)}{}_{,\theta z}\right) \\ + \ & d_{44}\left(u^{(n)}{}_{,rz} + \frac{1}{r}u^{(n)}{}_{,z} + \frac{1}{r}v^{(n)}{}_{,\theta z} + w^{(n)}{}_{,rr} + \frac{1}{r}w^{(n)}{}_{,r} + \frac{1}{r^2}w^{(n)}{}_{,\theta\theta}\right) \\ + \ & Q_3\left(U^{(n)}{}_{,rz} + \frac{1}{r}U^{(n)}{}_{,z} + \frac{1}{r}V^{(n)}{}_{,\theta z} + W^{(n)}{}_{,zz}\right) \\ = \ & -\omega^2\,\gamma_{11}^V\,w^{(n)} - \omega^2\,\gamma_{12}^V\,W^{(n)} \ , \end{aligned} \qquad (A-5.c)$$

$$
\begin{aligned}
& Q_1\left(u^{(n)}{}_{,rr}+\frac{1}{r}u^{(n)}{}_{,r}-\frac{1}{r^2}u^{(n)}+\frac{1}{r}v^{(n)}{}_{,\theta r}-\frac{1}{r^2}v^{(n)}{}_{,\theta}\right)+Q_3 w^{(n)}{}_{,rz} \\
+\ & \tilde{\mathcal{R}}\left(U^{(n)}{}_{,rr}+\frac{1}{r}U^{(n)}{}_{,r}-\frac{1}{r^2}U^{(n)}+\frac{1}{r}V^{(n)}{}_{,\theta r}-\frac{1}{r^2}V^{(n)}{}_{,\theta}+W^{(n)}{}_{,rz}\right) \qquad (A-5.d) \\
=\ & -\omega^2\,\gamma_{12}^H\,u^{(n)}-\omega^2\,\gamma_{22}^H\,U^{(n)}\,,
\end{aligned}
$$

$$
\begin{aligned}
& Q_1\left(\frac{1}{r}u^{(n)}{}_{,\theta r}+\frac{1}{r^2}u^{(n)}{}_{,\theta}+\frac{1}{r^2}v^{(n)}{}_{,\theta\theta}\right)+Q_3\frac{1}{r}w^{(n)}{}_{,\theta z} \\
+\ & \tilde{\mathcal{R}}\left(\frac{1}{r}U^{(n)}{}_{,\theta r}+\frac{1}{r^2}U^{(n)}{}_{,\theta}+\frac{1}{r^2}V^{(n)}{}_{,\theta\theta}+\frac{1}{r}W^{(n)}{}_{,\theta z}\right) \qquad (A-5.e) \\
=\ & -\omega^2\,\gamma_{12}^H\,v^{(n)}-\omega^2\,\gamma_{22}^H\,V^{(n)}\,,
\end{aligned}
$$

$$
\begin{aligned}
& Q_1\left(u^{(n)}{}_{,rz}+\frac{1}{r}u^{(n)}{}_{,z}+\frac{1}{r}v^{(n)}{}_{,\theta z}\right)+Q_3\,w^{(n)}{}_{,zz} \\
+\ & \tilde{\mathcal{R}}\left(U^{(n)}{}_{,rz}+\frac{1}{r}U^{(n)}{}_{,z}+\frac{1}{r}V^{(n)}{}_{,\theta z}+W^{(n)}{}_{,zz}\right) \qquad (A-5.f) \\
=\ & -\omega^2\,\gamma_{12}^V\,w^{(n)}-\omega^2\,\gamma_{22}^V\,W^{(n)}\,.
\end{aligned}
$$

Using the potential decomposition given in the text (Equ. (61) to (63)), the above equations can be written in a matrix form (Equ. (64)). The elements of the $\underline{\underline{\tilde{\mathcal{Z}}}}$ 6x6 complex matrix, noting

$$
\begin{aligned}
\mathcal{I}^{+(n)} &= I_{n+1}(q\,r)+I_{n-1}(q\,r)\,, \\
\mathcal{I}^{-(n)} &= I_{n+1}(q\,r)-I_{n-1}(q\,r)\,,
\end{aligned}
$$

and assuming that neither $I_n(q\,r)$ or $\mathcal{I}^{+(n)}$ or $\mathcal{I}^{-(n)}$ is equal to 0, are:

$$
\begin{aligned}
\tilde{\mathcal{Z}}_{11} &= \left\{d_{11}\,q^2-(d_{13}+2\,d_{44})\,k^2+\omega^2\gamma_{11}^H\right\}\mathcal{I}^{+(n)}\,, \\
\tilde{\mathcal{Z}}_{12} &= \left\{d_{44}\,k^2-d_{66}\,q^2-\omega^2\,\gamma_{11}^H\right\}\mathcal{I}^{-(n)}\,, \\
\tilde{\mathcal{Z}}_{13} &= ik\left\{(d_{11}-d_{13})\,q^2-d_{44}\,(k^2+q^2)+\omega^2\,\gamma_{11}^H\right\}\mathcal{I}^{+(n)}\,, \qquad (A-6.a) \\
\tilde{\mathcal{Z}}_{14} &= \left\{Q_1\,(q^2-k^2)+\omega^2\,\gamma_{12}^H\right\}\mathcal{I}^{+(n)}\,, \\
\tilde{\mathcal{Z}}_{15} &= -\omega^2\,\gamma_{12}^H\,\mathcal{I}^{-(n)}\,, \\
\tilde{\mathcal{Z}}_{16} &= ik\,\omega^2\,\gamma_{12}^H\,\mathcal{I}^{+(n)}\,;
\end{aligned}
$$

$$
\begin{aligned}
\tilde{\mathcal{Z}}_{21} &= \left\{d_{11}\,q^2-(d_{13}+2\,d_{44})\,k^2+\omega^2\gamma_{11}^H\right\}\mathcal{I}^{-(n)}\,, \\
\tilde{\mathcal{Z}}_{22} &= \left\{d_{44}\,k^2-d_{66}\,q^2-\omega^2\,\gamma_{11}^H\right\}\mathcal{I}^{+(n)}\,, \\
\tilde{\mathcal{Z}}_{23} &= ik\left\{(d_{11}-d_{13})\,q^2-d_{44}\,(k^2+q^2)+\omega^2\,\gamma_{11}^H\right\}\mathcal{I}^{-(n)}\,, \qquad (A-6.b) \\
\tilde{\mathcal{Z}}_{24} &= \left\{Q_1\,(q^2-k^2)+\omega^2\,\gamma_{12}^H\right\}\mathcal{I}^{-(n)}\,, \\
\tilde{\mathcal{Z}}_{25} &= -\omega^2\,\gamma_{12}^H\,\mathcal{I}^{+(n)}\,, \\
\tilde{\mathcal{Z}}_{26} &= ik\,\omega^2\,\gamma_{12}^H\,\mathcal{I}^{-(n)}\,;
\end{aligned}
$$

$$
\begin{aligned}
\tilde{\mathcal{Z}}_{31} &= ik\left\{-d_{33}\,k^2+q^2\,(d_{13}+2\,d_{44})+\omega^2\,\gamma_{11}^V\right\}\,,\\
\tilde{\mathcal{Z}}_{32} &= 0\,,\\
\tilde{\mathcal{Z}}_{33} &= q^2\left\{k^2\,(d_{33}-d_{44}-d_{13})-q^2\,d_{44}-\omega^2\,\gamma_{11}^V\right\}\,,\\
\tilde{\mathcal{Z}}_{34} &= ik\left\{Q_3\,(q^2-k^2)+\omega^2\,\gamma_{12}^V\right\}\,,\\
\tilde{\mathcal{Z}}_{35} &= 0\,,\\
\tilde{\mathcal{Z}}_{36} &= -q^2\,\omega^2\,\gamma_{12}^V\,;
\end{aligned}
\qquad (\mathrm{A}-6.\mathrm{c})
$$

$$
\begin{aligned}
\tilde{\mathcal{Z}}_{41} &= \left\{Q_1\,q^2-Q_3\,k^2+\omega^2\,\gamma_{12}^H\right\}\mathcal{I}^{+(n)}\,,\\
\tilde{\mathcal{Z}}_{42} &= -\omega^2\,\gamma_{12}^H\,\mathcal{I}^{-(n)}\,,\\
\tilde{\mathcal{Z}}_{43} &= ik\left\{q^2\,(Q_1-Q_3)+\omega^2\,\gamma_{12}^H\right\}\mathcal{I}^{+(n)}\,,\\
\tilde{\mathcal{Z}}_{44} &= \left\{\tilde{\mathcal{R}}\,(q^2-k^2)+\omega^2\,\gamma_{22}^H\right\}\mathcal{I}^{+(n)}\,,\\
\tilde{\mathcal{Z}}_{45} &= -\omega^2\,\gamma_{22}^H\,\mathcal{I}^{-(n)}\,,\\
\tilde{\mathcal{Z}}_{46} &= ik\,\omega^2\,\gamma_{22}^H\,\mathcal{I}^{+(n)}\,;
\end{aligned}
\qquad (\mathrm{A}-6.\mathrm{d})
$$

$$
\begin{aligned}
\tilde{\mathcal{Z}}_{51} &= \left\{Q_1\,q^2-Q_3\,k^2+\omega^2\,\gamma_{12}^H\right\}\mathcal{I}^{-(n)}\,,\\
\tilde{\mathcal{Z}}_{52} &= -\omega^2\,\gamma_{12}^H\,\mathcal{I}^{+(n)}\,,\\
\tilde{\mathcal{Z}}_{53} &= ik\left\{q^2\,(Q_1-Q_3)+\omega^2\,\gamma_{12}^H\right\}\mathcal{I}^{-(n)}\,,\\
\tilde{\mathcal{Z}}_{54} &= \left\{\tilde{\mathcal{R}}\,(q^2-k^2)+\omega^2\,\gamma_{22}^H\right\}\mathcal{I}^{-(n)}\,,\\
\tilde{\mathcal{Z}}_{55} &= -\omega^2\,\gamma_{22}^H\,\mathcal{I}^{+(n)}\,,\\
\tilde{\mathcal{Z}}_{56} &= ik\,\omega^2\,\gamma_{22}^H\,\mathcal{I}^{-(n)}\,;
\end{aligned}
\qquad (\mathrm{A}-6.\mathrm{e})
$$

$$
\begin{aligned}
\tilde{\mathcal{Z}}_{61} &= ik\left\{Q_1\,q^2-Q_3\,k^2+\omega^2\,\gamma_{12}^V\right\}\,,\\
\tilde{\mathcal{Z}}_{62} &= 0\,,\\
\tilde{\mathcal{Z}}_{63} &= q^2\left\{(Q_3-Q_1)\,k^2-\omega^2\,\gamma_{12}^V\right\}\,,\\
\tilde{\mathcal{Z}}_{64} &= ik\left\{\tilde{\mathcal{R}}\,(q^2-k^2)+\omega^2\,\gamma_{22}^V\right\}\,,\\
\tilde{\mathcal{Z}}_{65} &= 0\,,\\
\tilde{\mathcal{Z}}_{66} &= -q^2\,\omega^2\,\gamma_{22}^V\,.
\end{aligned}
\qquad (\mathrm{A}-6.\mathrm{f})
$$

SH wave

Although apparently complicated, the expression of Det $\left(\underline{\underline{\tilde{\mathcal{Z}}}}\right)$ can be greatly simplified by performing some algebraic manipulations. When Row 1 and Row 4 are respectively replaced by (Row 1 - Row 2), and (Row 4 - Row 5), the terms $\mathcal{I}^{+(n)}$ and $\mathcal{I}^{-(n)}$ (in fact, combinations of thereof) can be factorized from those two rows. The remaining terms are then respectively multiplied by (+1, −1, +1, +1, −1, +1). The fifth and second rows being replaced by (Row 2 - $\mathcal{I}^{-(n)}$ Row 1) and (Row 5 - $\mathcal{I}^{-(n)}$ Row 4), the

modified fifth row yields the weighting coefficient $\tilde{C}_f^{(n)}$ of the horizontally polarized shear potential of the fluid (Equ. (65)). The corresponding radial wavenumber (Equ. (66)) is obtained by introducing this relation into the modified second row.

Quasi body waves

Skipping the second and fifth rows and columns from the last obtained determinant, the elements ζ_{kl} of the new 4x4 complex matrix $\underline{\underline{\tilde{Z}}}$ are:

$$\begin{aligned}
\zeta_{11} &= d_{11}\,q^2 - (d_{13} + 2\,d_{44})\,k^2 + \omega^2\gamma_{11}^H\,, \\
\zeta_{12} &= ik\left\{(d_{11} - d_{13})\,q^2 - d_{44}\,(k^2 + q^2) + \omega^2\,\gamma_{11}^H\right\}\,, \\
\zeta_{13} &= Q_1\,(q^2 - k^2) + \omega^2\,\gamma_{12}^H\,, \\
\zeta_{14} &= ik\,\omega^2\,\gamma_{12}^H\,;
\end{aligned} \qquad (\mathrm{A}-7.\mathrm{a})$$

$$\begin{aligned}
\zeta_{21} &= ik\left\{-d_{33}\,k^2 + q^2\,(d_{13} + 2\,d_{44}) + \omega^2\,\gamma_{11}^V\right\}\,, \\
\zeta_{22} &= q^2\left\{k^2\,(d_{33} - d_{44} - d_{13}) - q^2\,d_{44} - \omega^2\,\gamma_{11}^V\right\}\,, \\
\zeta_{23} &= ik\left\{Q_3\,(q^2 - k^2) + \omega^2\,\gamma_{12}^V\right\}\,, \\
\zeta_{24} &= -q^2\,\omega^2\,\gamma_{12}^V\,;
\end{aligned} \qquad (\mathrm{A}-7.\mathrm{b})$$

$$\begin{aligned}
\zeta_{31} &= Q_1\,q^2 - Q_3\,k^2 + \omega^2\,\gamma_{12}^H\,, \\
\zeta_{32} &= ik\left\{q^2\,(Q_1 - Q_3) + \omega^2\,\gamma_{12}^H\right\}\,, \\
\zeta_{33} &= \tilde{\mathcal{R}}\,(q^2 - k^2) + \omega^2\,\gamma_{22}^H\,, \\
\zeta_{34} &= ik\,\omega^2\,\gamma_{22}^H\,;
\end{aligned} \qquad (\mathrm{A}-7.\mathrm{c})$$

$$\begin{aligned}
\zeta_{41} &= ik\left\{Q_1\,q^2 - Q_3\,k^2 + \omega^2\,\gamma_{12}^V\right\}\,, \\
\zeta_{42} &= q^2\left\{(Q_3 - Q_1)\,k^2 - \omega^2\,\gamma_{12}^V\right\}\,, \\
\zeta_{43} &= ik\left\{\tilde{\mathcal{R}}\,(q^2 - k^2) + \omega^2\,\gamma_{22}^V\right\}\,, \\
\zeta_{44} &= -q^2\,\omega^2\,\gamma_{22}^V\,.
\end{aligned} \qquad (\mathrm{A}-7.\mathrm{d})$$

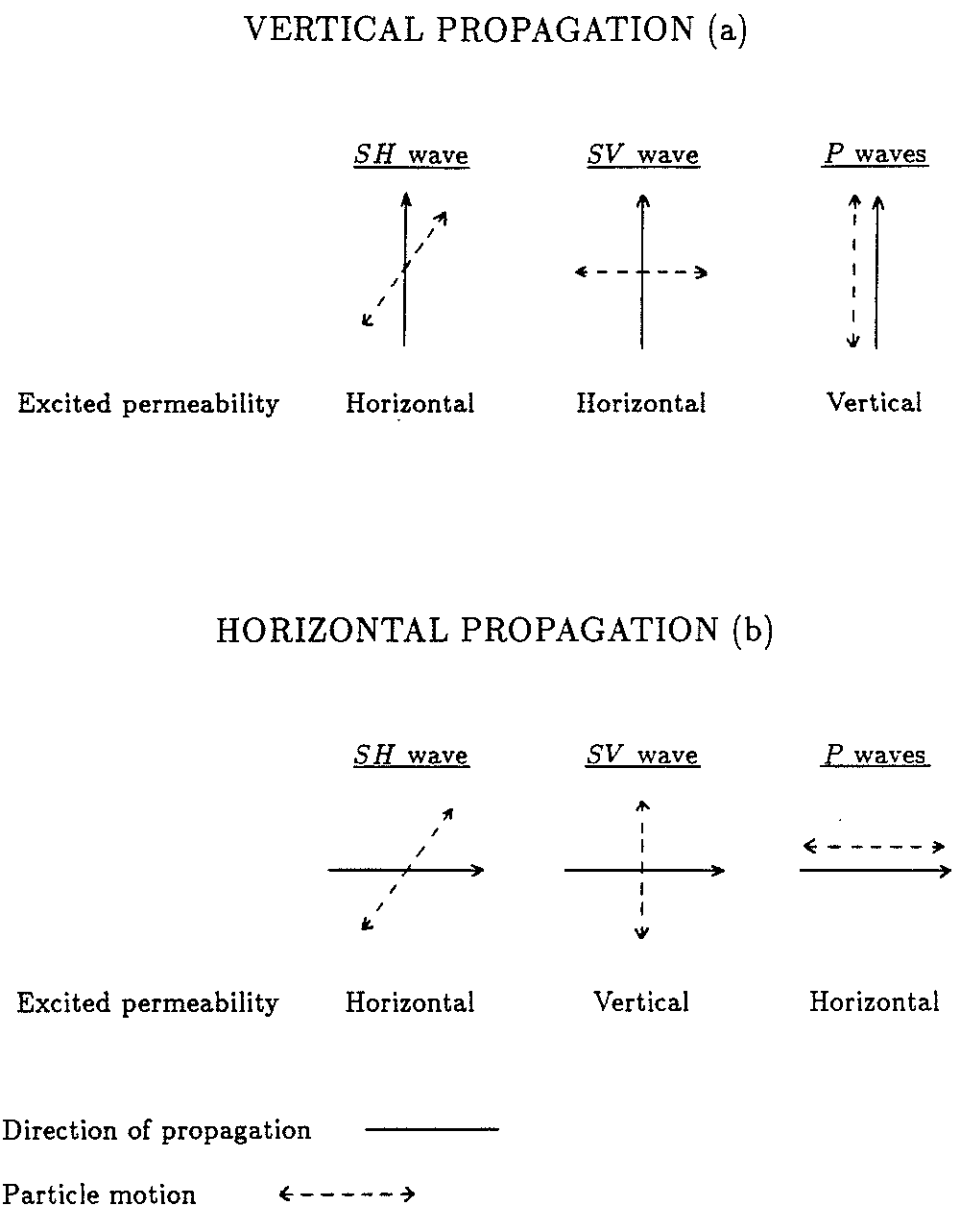

Figure 1: First order "geometric interpretation" of the permeability excited by the SH wave, the quasi SV wave, and both compressional waves for vertical (a) and horizontal (b) propagation.

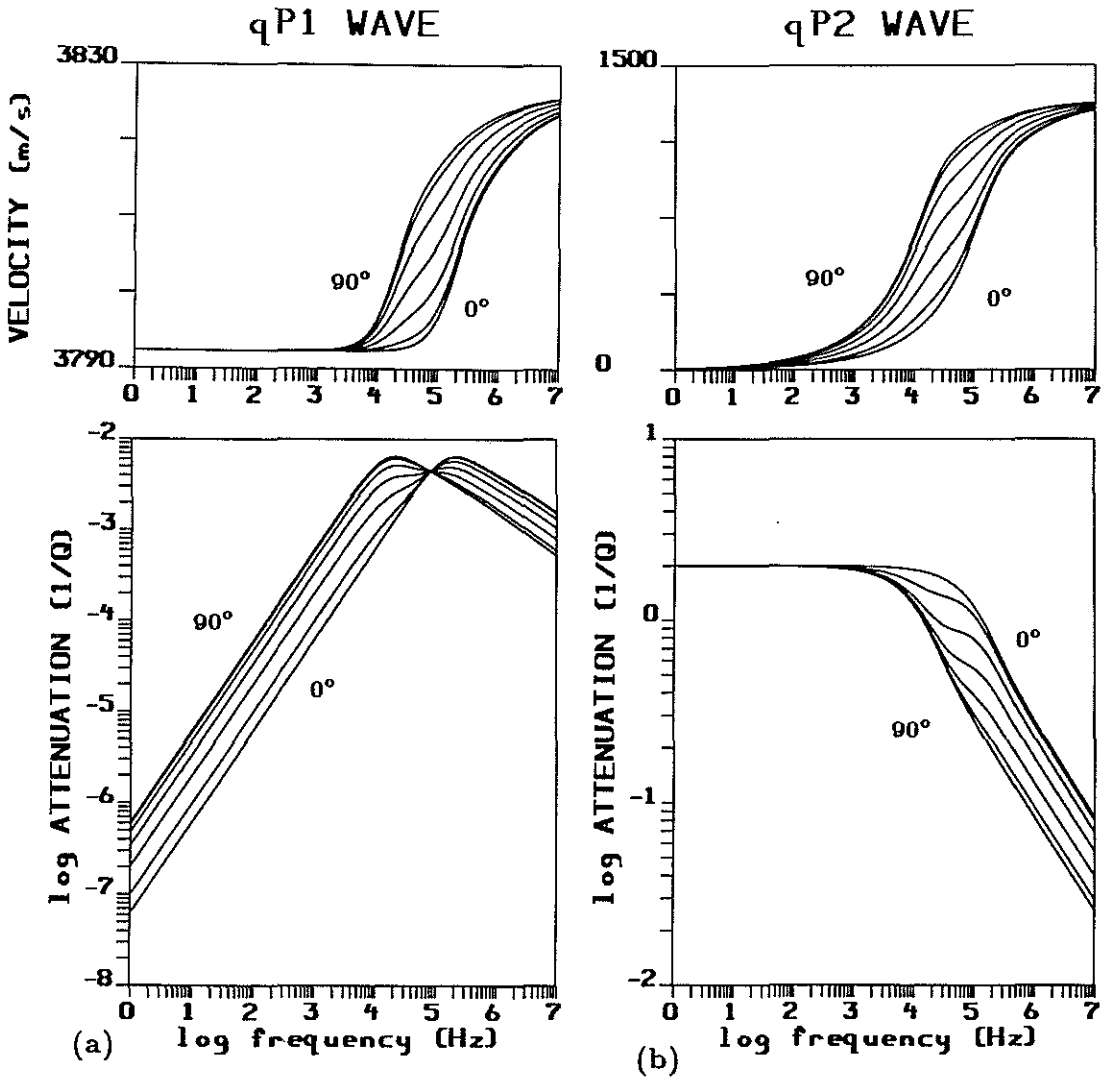

Figure 2: Effects of the only transversely isotropic permeability. Phase velocity and attenuation $(1/Q)$ as a function of frequency of the quasi P_1-wave (a), the quasi P_2-wave (b), the quasi SV-wave (c) and the SH-wave (d) which propagate in a fast sandstone (see Table 1). The pores are straight cylindrical ducts (i.e., $\tilde{\tau}^H = \tilde{\tau}^V = 1$). For each wave, the different curves corresponds to values of the angle of propagation with respect to the vertical which varies from 0^o to 90^o by step of 15^o. Also displayed are the curves associated with a 1 darcy and a 100 mdarcies isotropic permeability. For both quasi compressional waves, they are identical to the curves obtained with a horizontal and a vertical propagation, respectively. The correspondance is reverse for the quasi SV wave. For the SH wave, the 1 darcy isotropic permeability curve corresponds to those obtained with the only transversely isotropic permeability situation, whatever the angle of propagation (see text).

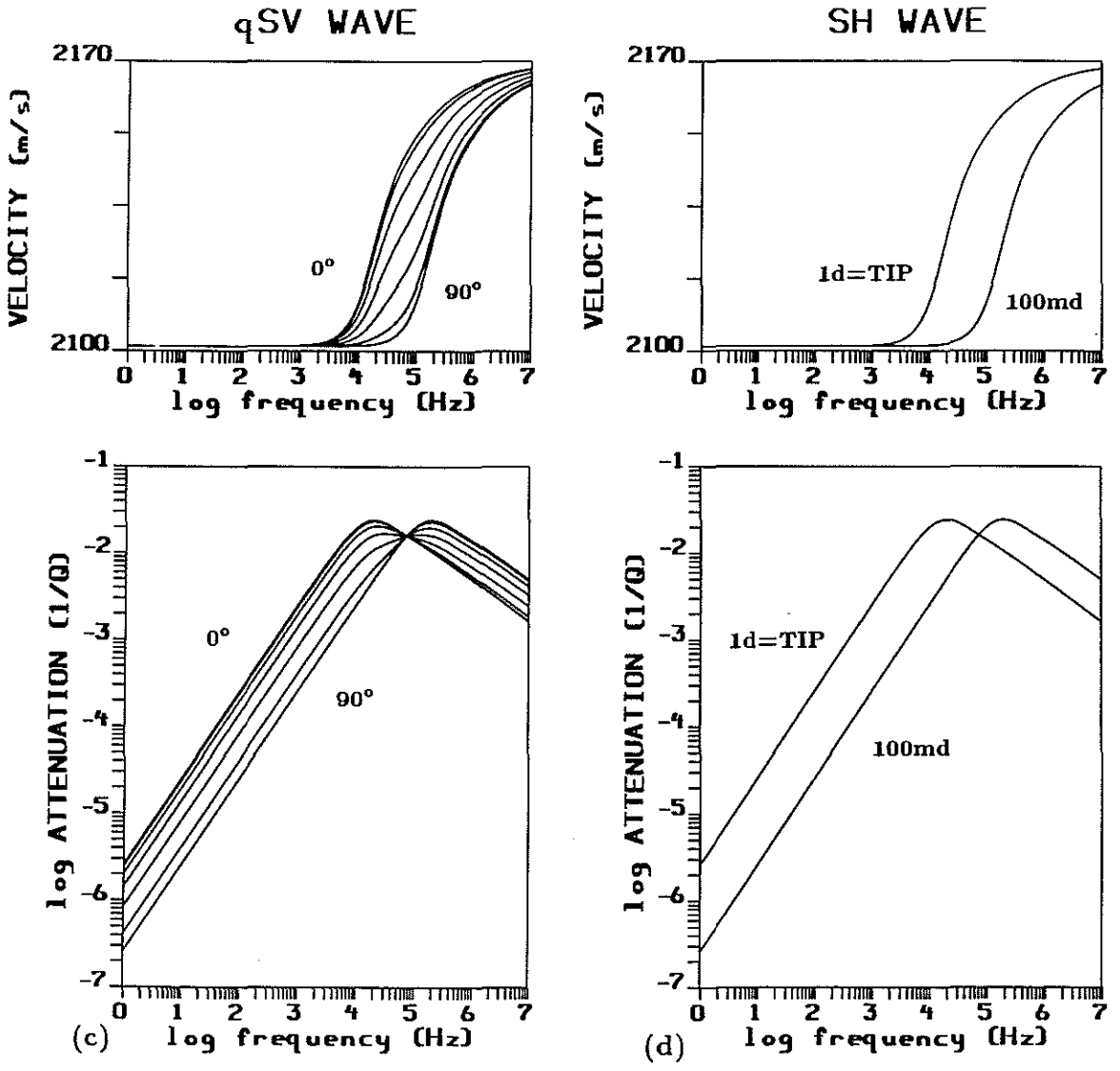
qSV WAVE
SH WAVE
VELOCITY (m/s)
2170
2100
0°
90°
1d=TIP
100md
0 1 2 3 4 5 6 7
log frequency (Hz)
log ATTENUATION (1/Q)
-1
-2
-3
-4
-5
-6
-7
(c)
(d)

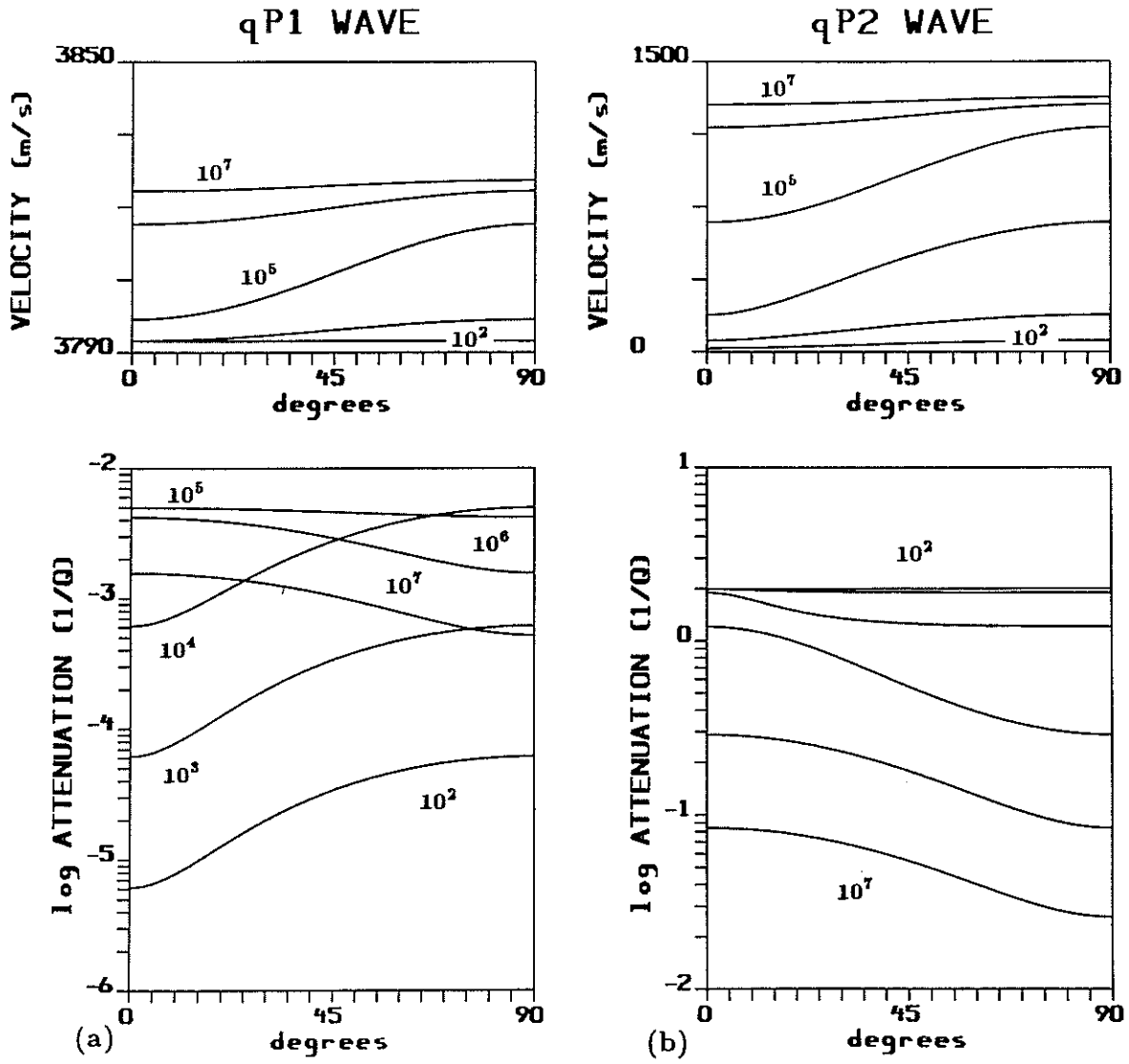

Figure 3: Same as Figure 2 but as a function of the angle of propagation with respect to the vertical. For each wave, the different curves correspond to values of the frequency indicated in Hz. The isotropic permeability situations are omitted.

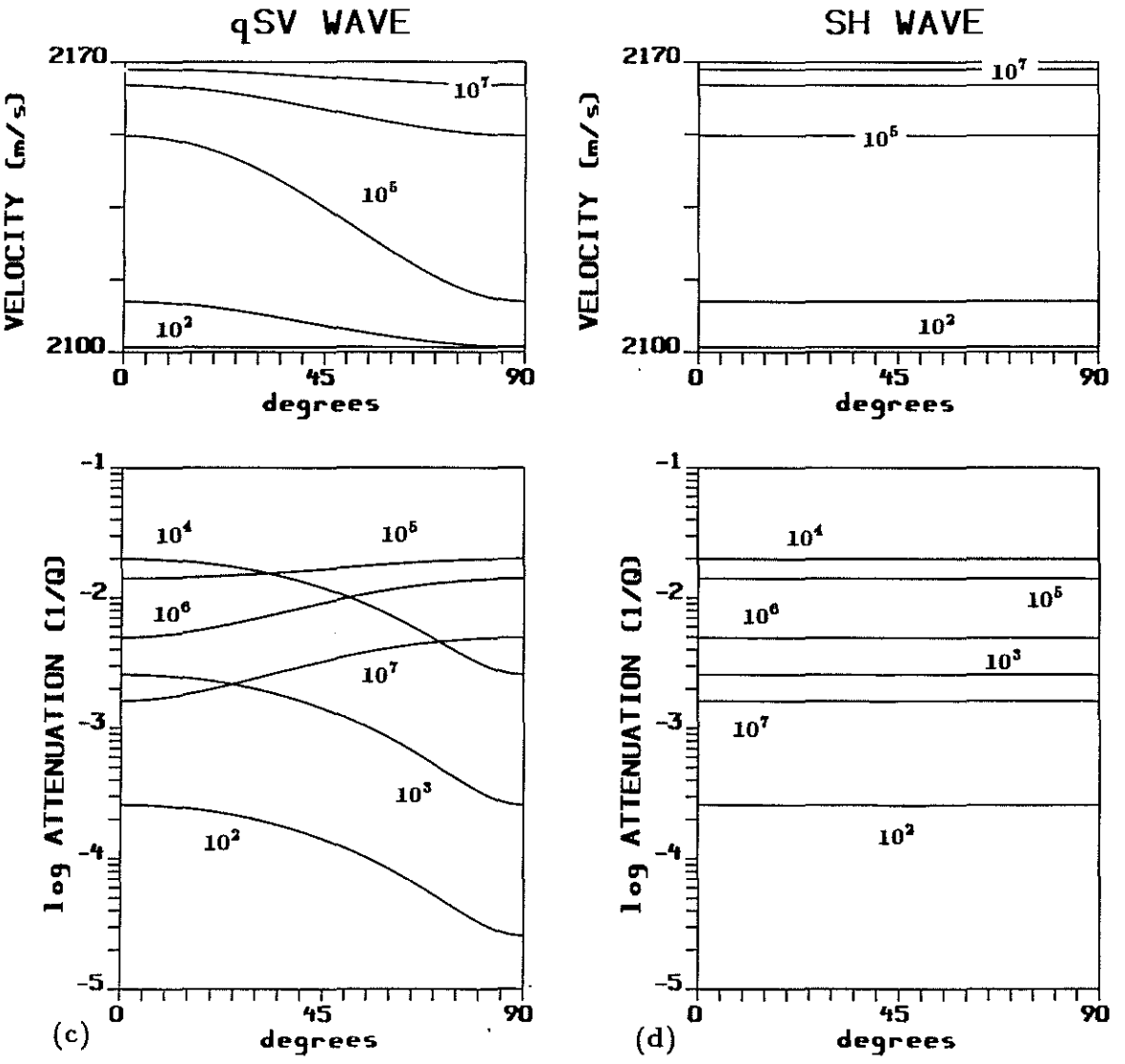
qSV WAVE
SH WAVE
VELOCITY (m/s)
2170
2100
10^7
10^5
10^2
0
45
90
degrees
log ATTENUATION (1/Q)
-1
-2
-3
-4
-5
10^4
10^6
10^3
(c)
(d)

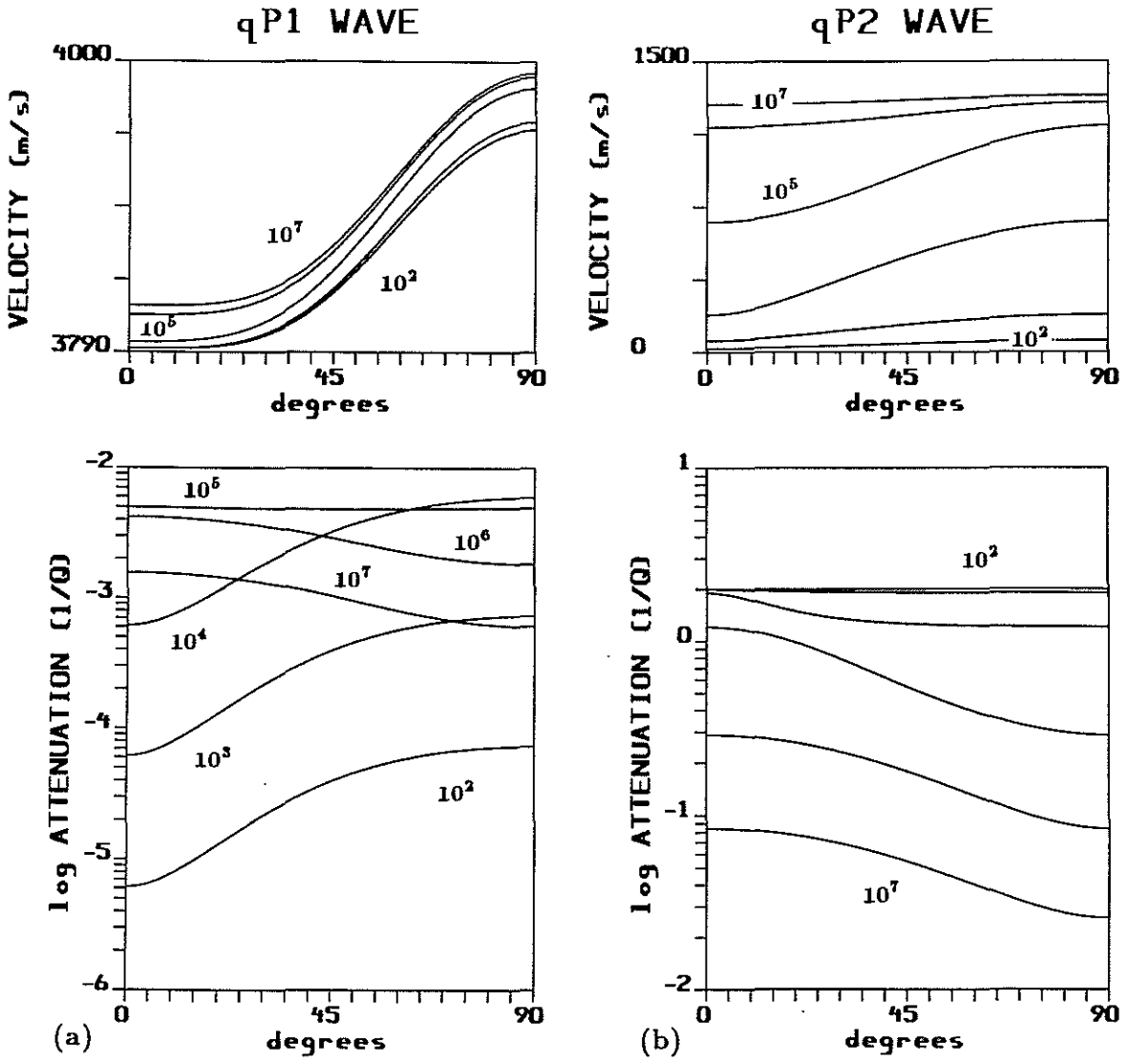

Figure 4: Same as Figure 3 but when the skeleton is transversely isotropic (see Table 1). Note the difference in the horizontally and vertically propagating SV-wave velocities in the intermediate frequency range (i.e., $\simeq 10^5 Hz$).

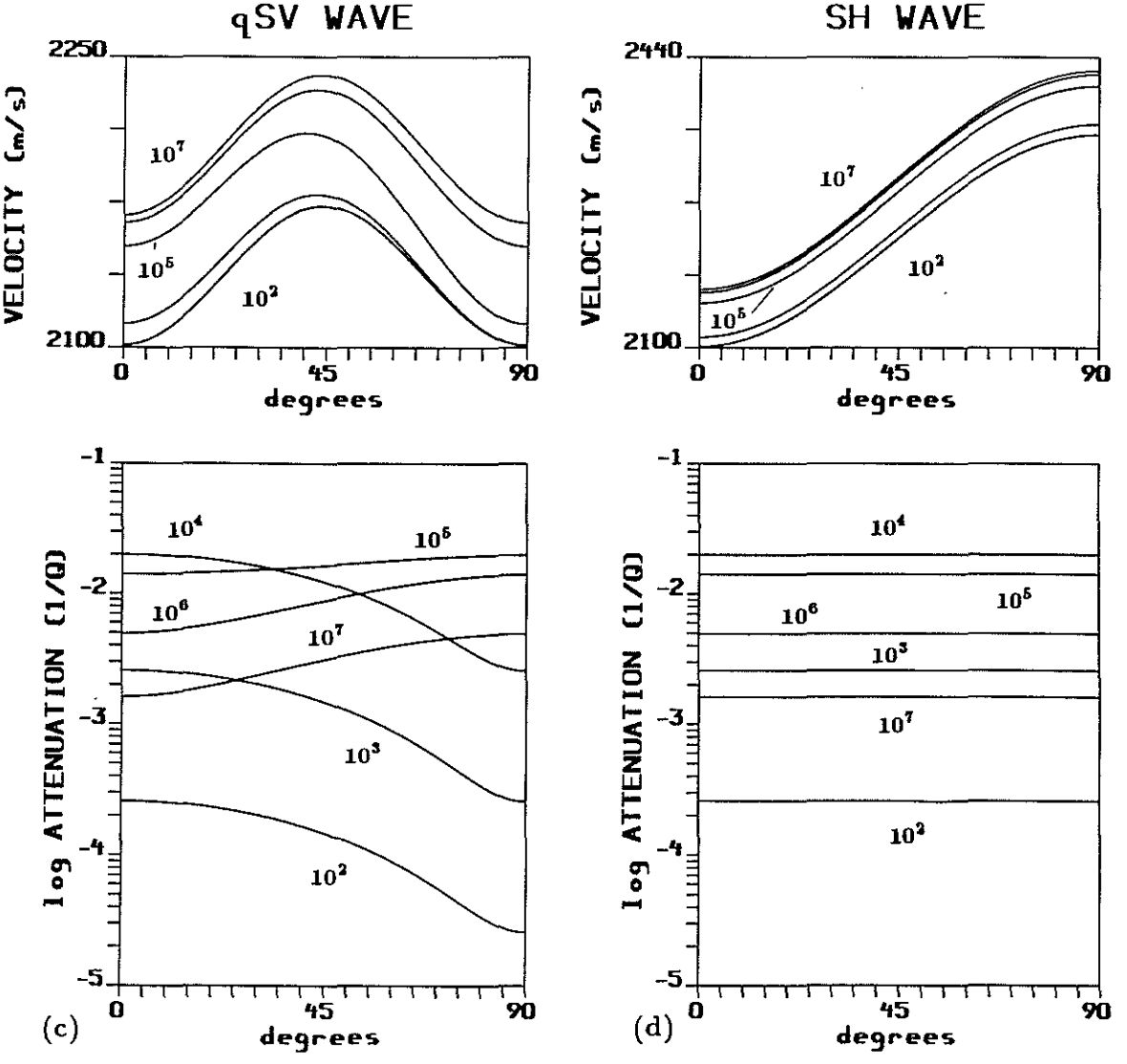
qSV WAVE
SH WAVE
VELOCITY (m/s)
2250
2100
2440
2100
10^7
10^5
10^2
10^4
10^6
10^3
0
45
90
degrees
log ATTENUATION (1/Q)
-1
-2
-3
-4
-5
(c)
(d)

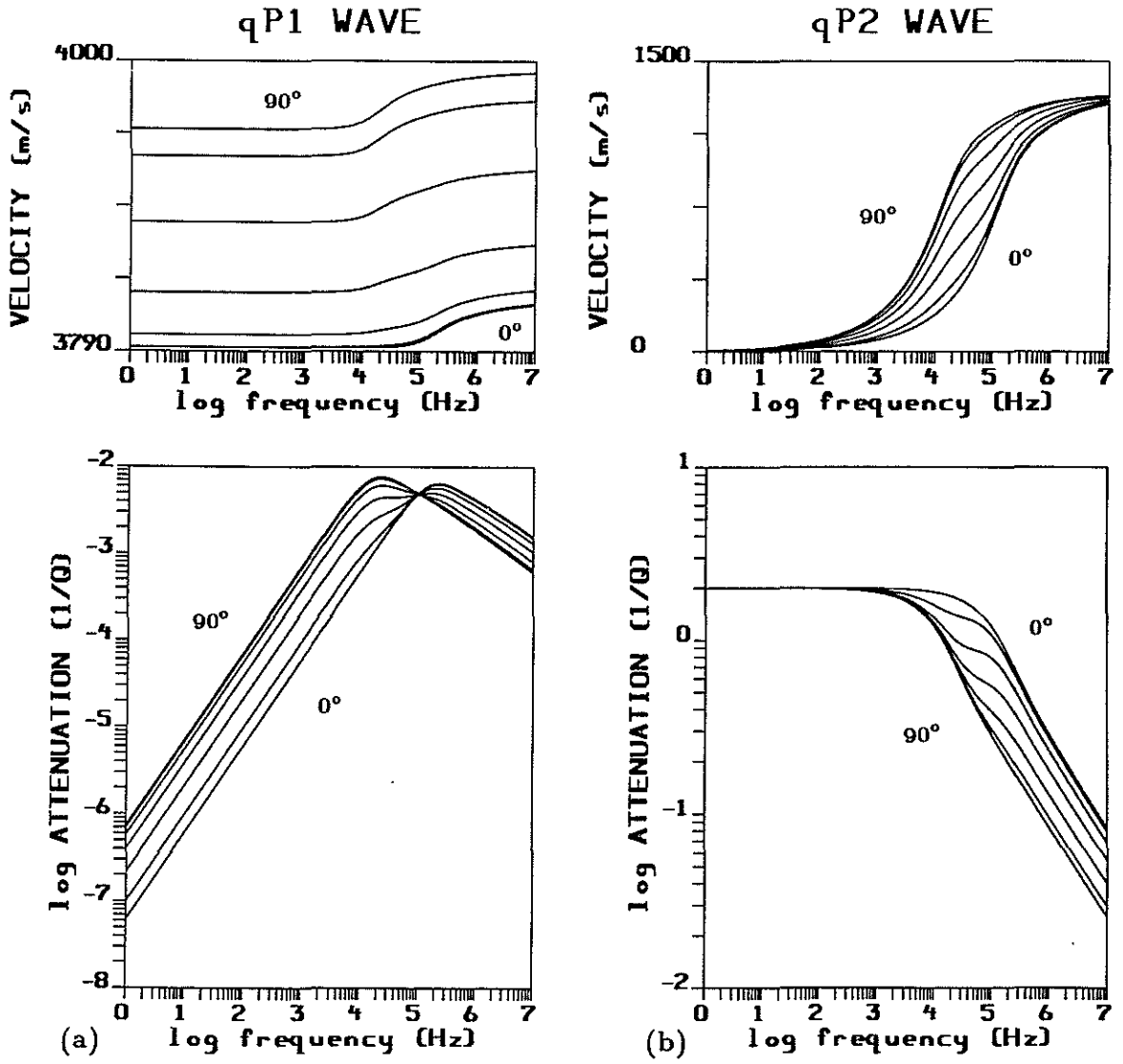

Figure 5: Transversely isotropic saturated porous sandstone (see Table 1). Phase velocity and attenuation ($1/Q$) as a function of frequency of the quasi P_1-wave (a), the quasi P_2-wave (b), the quasi SV-wave (c) and the SH-wave (d). For each wave, the different curves corresponds to values of the angle of propagation with respect to the vertical which varies from $0°$ to $90°$ by step of $15°$. Compare with Figure 2 (the isotropic permeability situations are omitted).

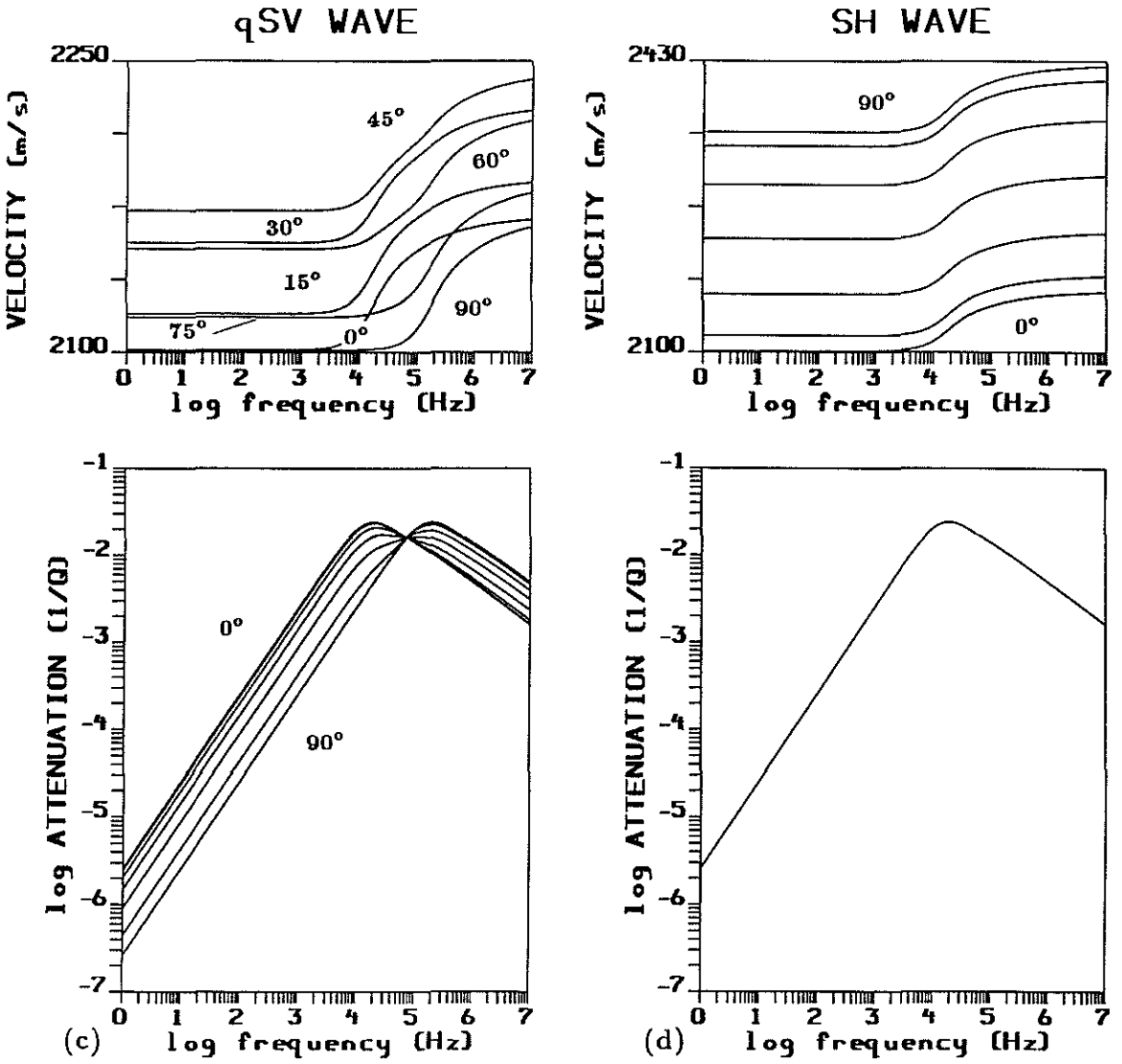
qSV WAVE
SH WAVE
VELOCITY (m/s)
2250
2100
2430
2100
45°
60°
30°
15°
75°
0°
90°
90°
0°
0 1 2 3 4 5 6 7
log frequency (Hz)
log ATTENUATION (1/Q)
-1
-2
-3
-4
-5
-6
-7
0°
90°
(c)
(d)

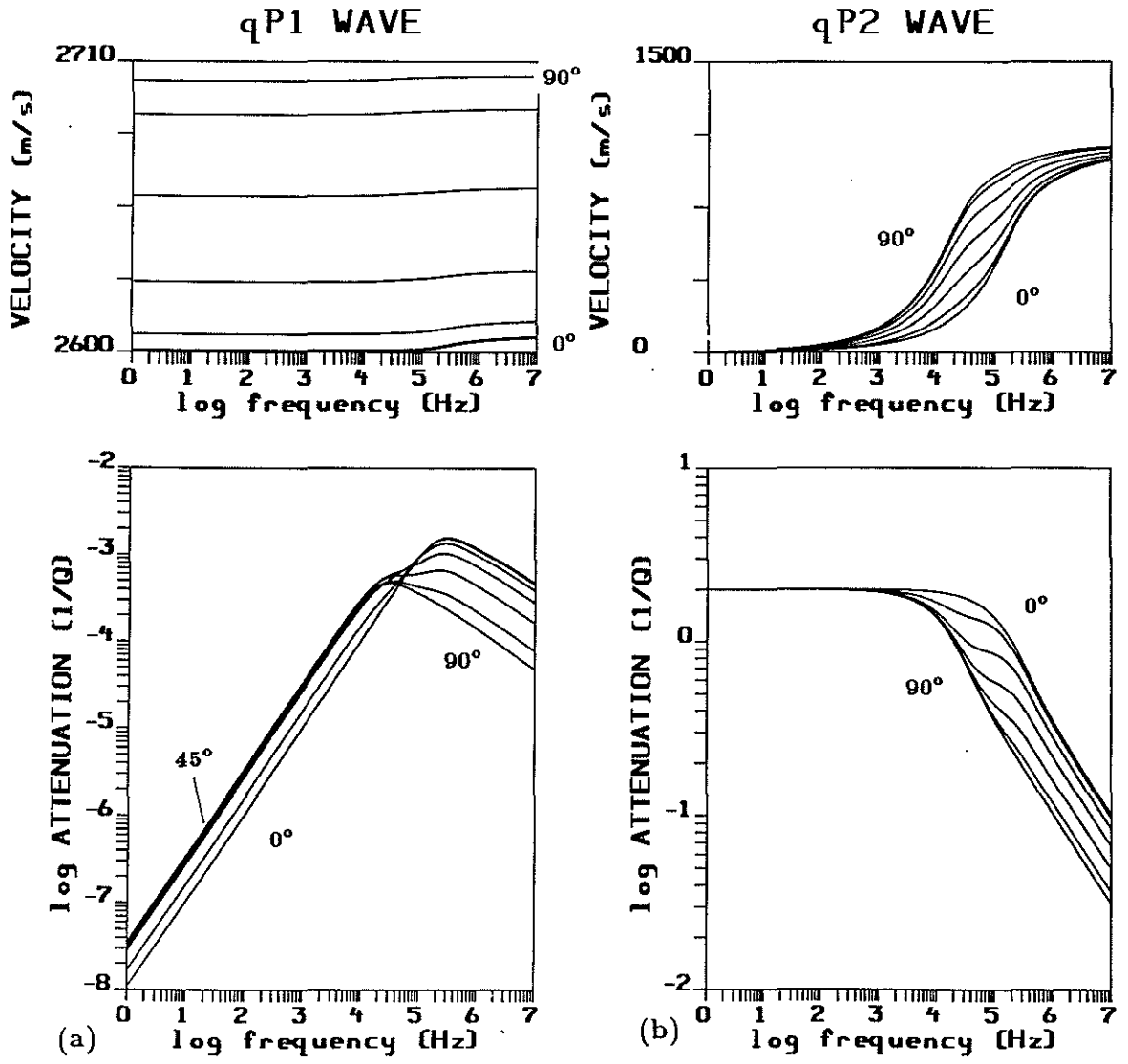

Figure 6: Same as Figure 5 for a transversly isotropic "softer" formation (see Table 1). Note the variations of the quasi P_1-wave attenuations.

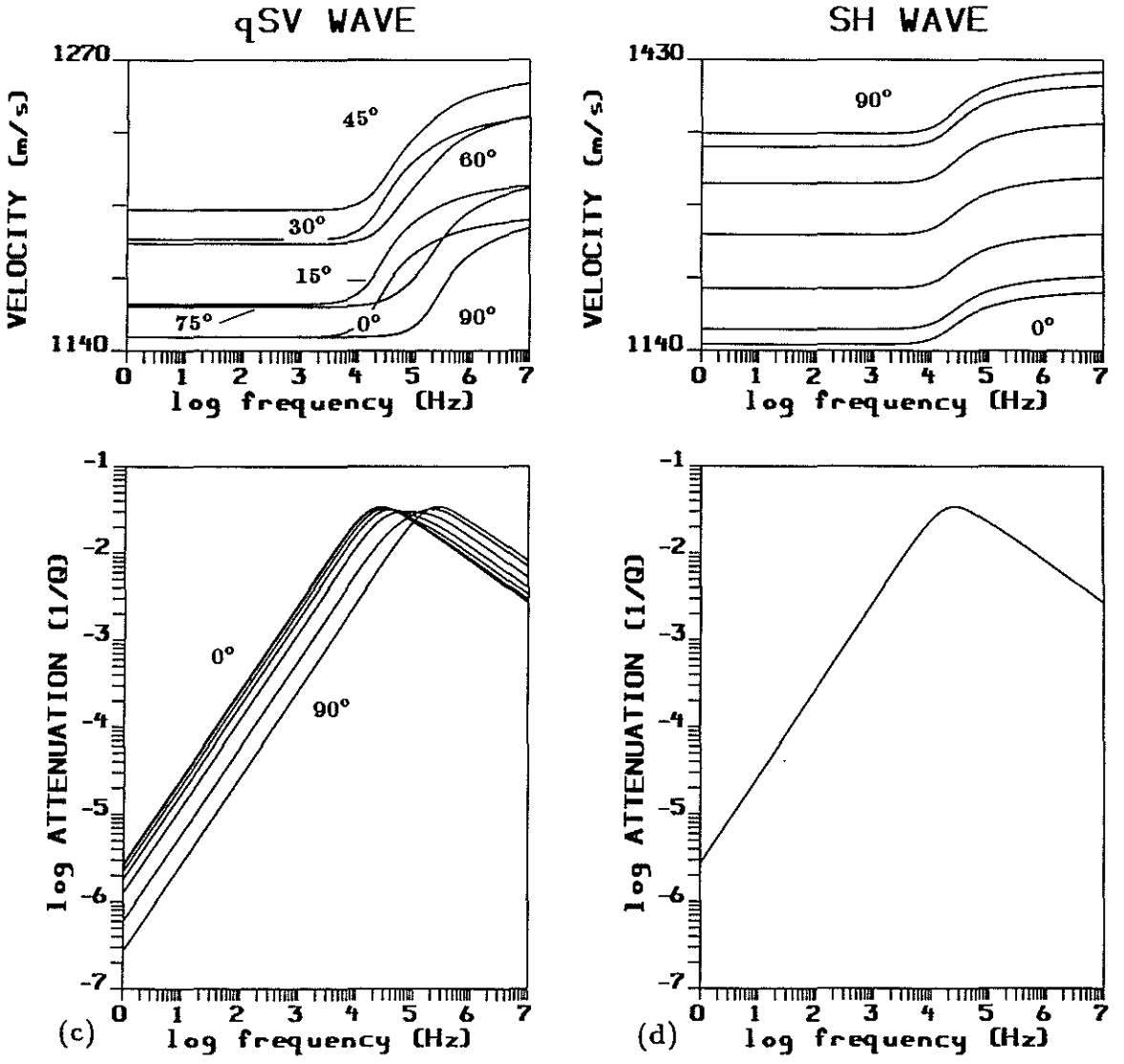
qSV WAVE
SH WAVE
VELOCITY (m/s)
1270
1140
1430
1140
45°
60°
30°
15°
75°
0°
90°
90°
0°
0 1 2 3 4 5 6 7
log frequency (Hz)
log ATTENUATION (1/Q)
-1
-2
-3
-4
-5
-6
-7
0°
90°
(c)
(d)

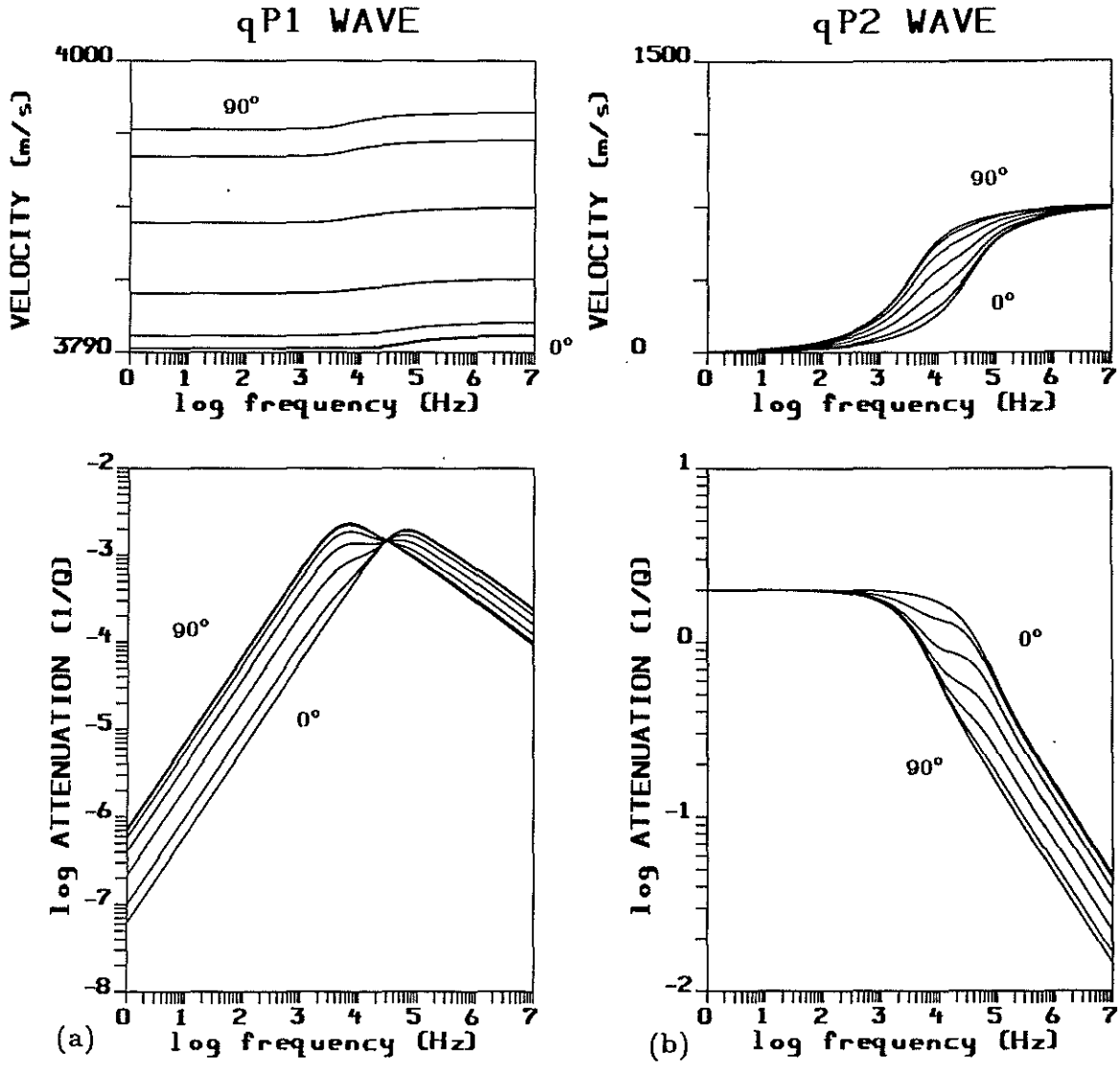

Figure 7: Mass coupling coefficient (tortuosity) effects. Same as Figure 4 but with both horizontal and vertical tortuosities equal to 3.

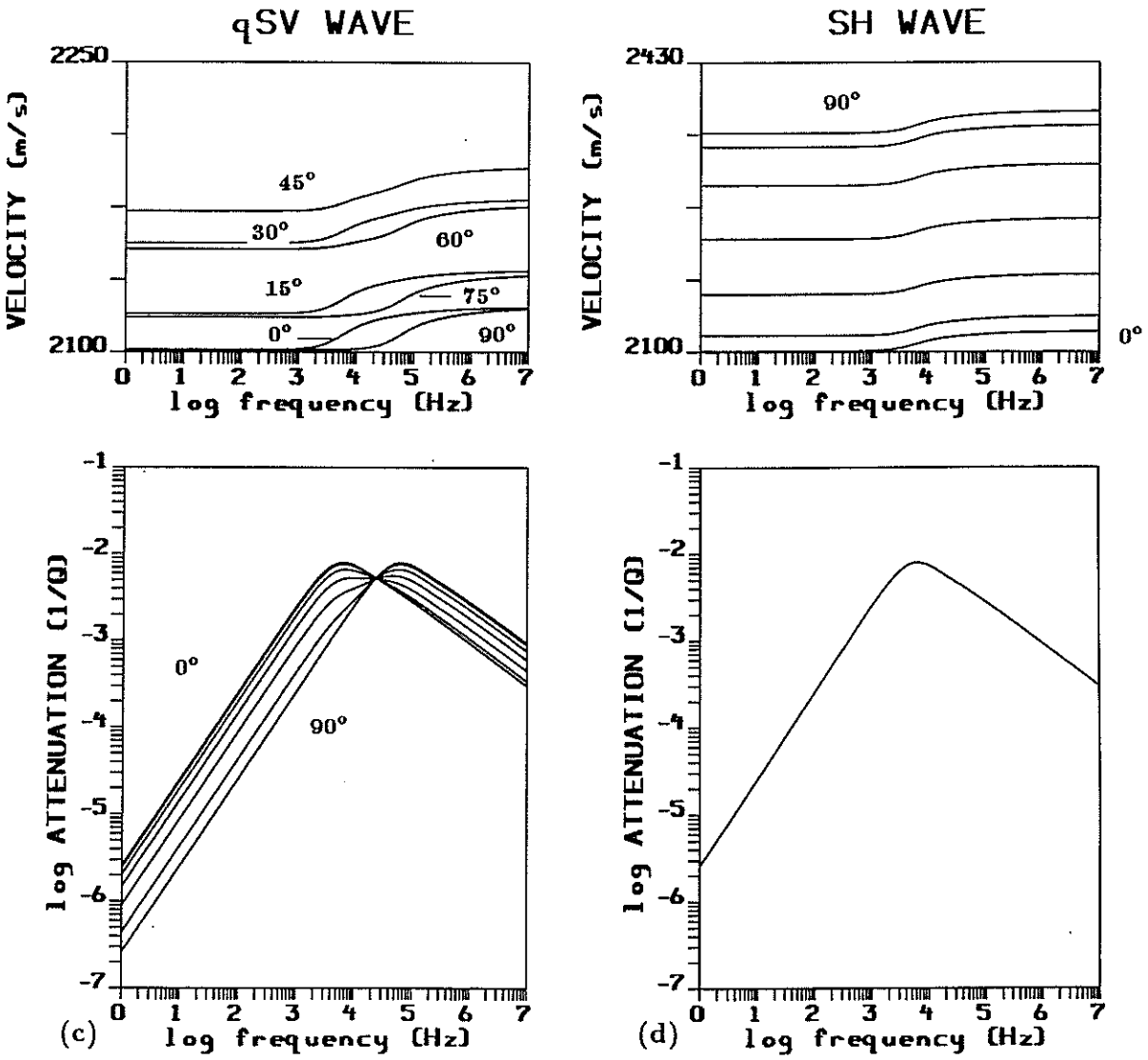
qSV WAVE
SH WAVE
VELOCITY (m/s)
2250
2100
2430
45°
30°
60°
15°
75°
0°
90°
log frequency (Hz)
log ATTENUATION (1/Q)
(c)
(d)

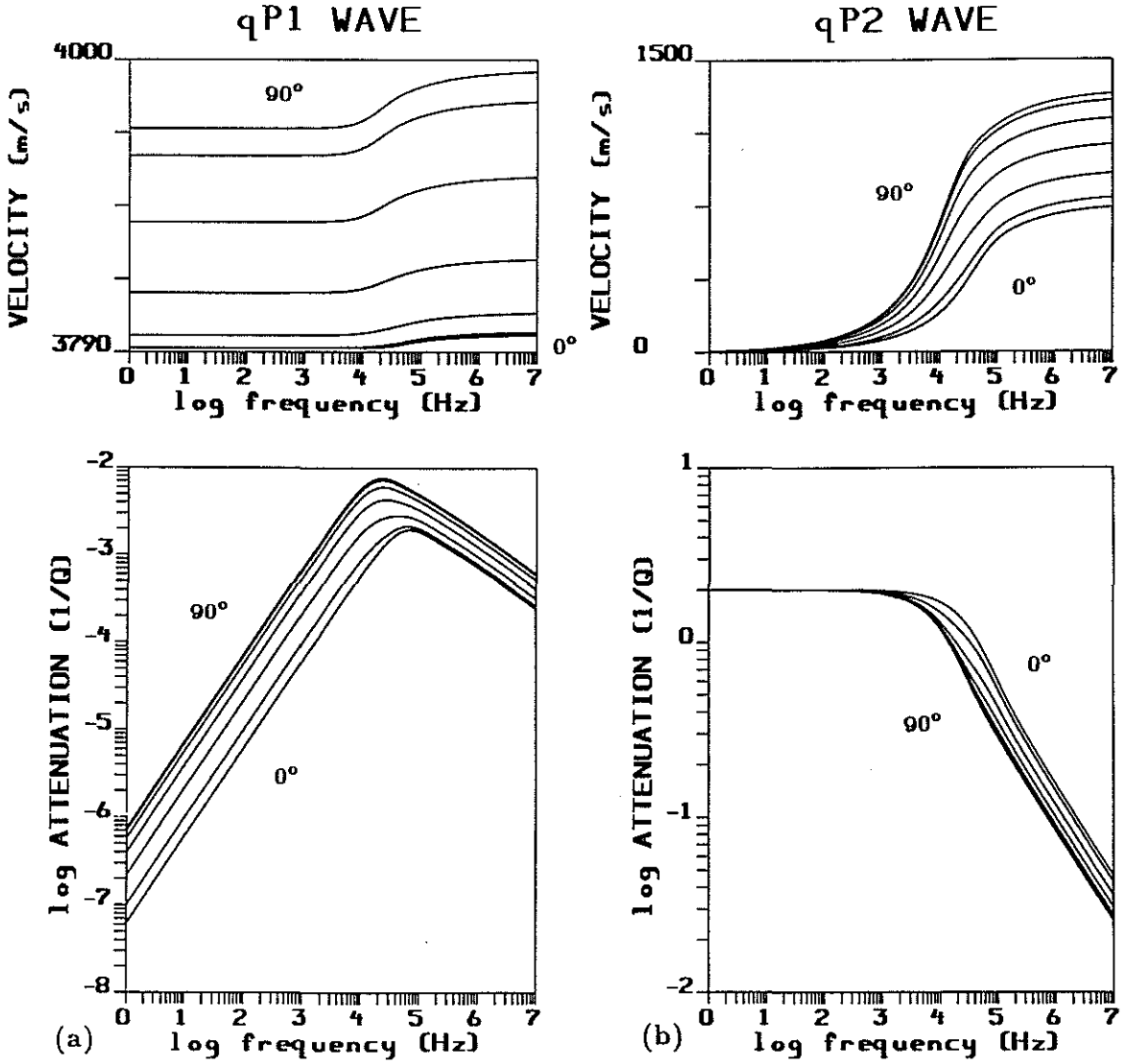

Figure 8: Anisotropic mass coupling coefficient (tortuosity) effects. Same as Figures 7 and 4 but with a unit horizontal tortuosity and and a vertical tortuosity equal to 3. Note the high frequency variations of the quasi slow P_2-wave velocity (b).

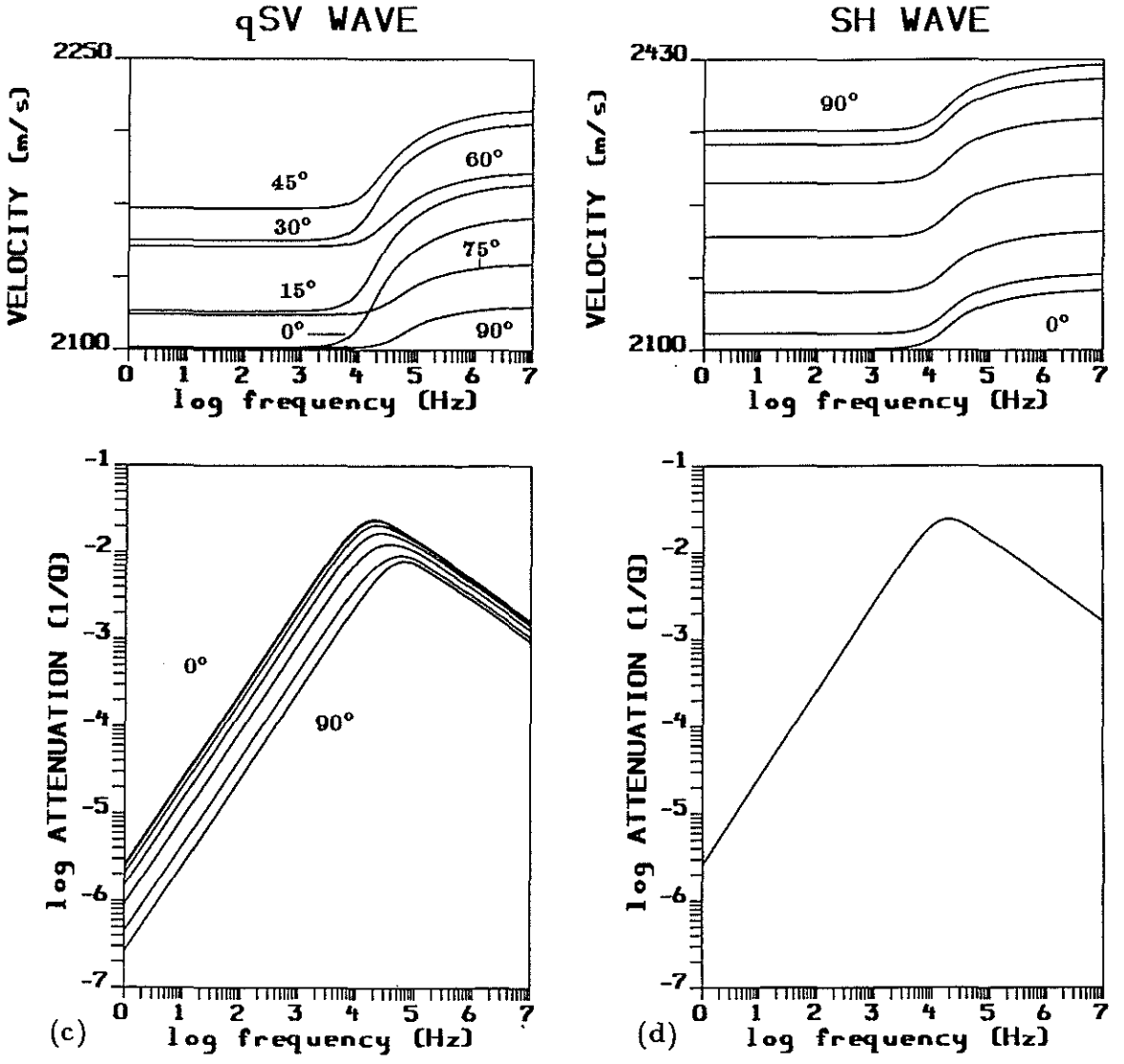
qSV WAVE
SH WAVE
VELOCITY (m/s)
2250
2100
2430
2100
45°
60°
30°
75°
15°
0°
90°
90°
0°
0 1 2 3 4 5 6 7
log frequency (Hz)
log ATTENUATION (1/Q)
-1
-2
-3
-4
-5
-6
-7
0°
90°
(c)
(d)

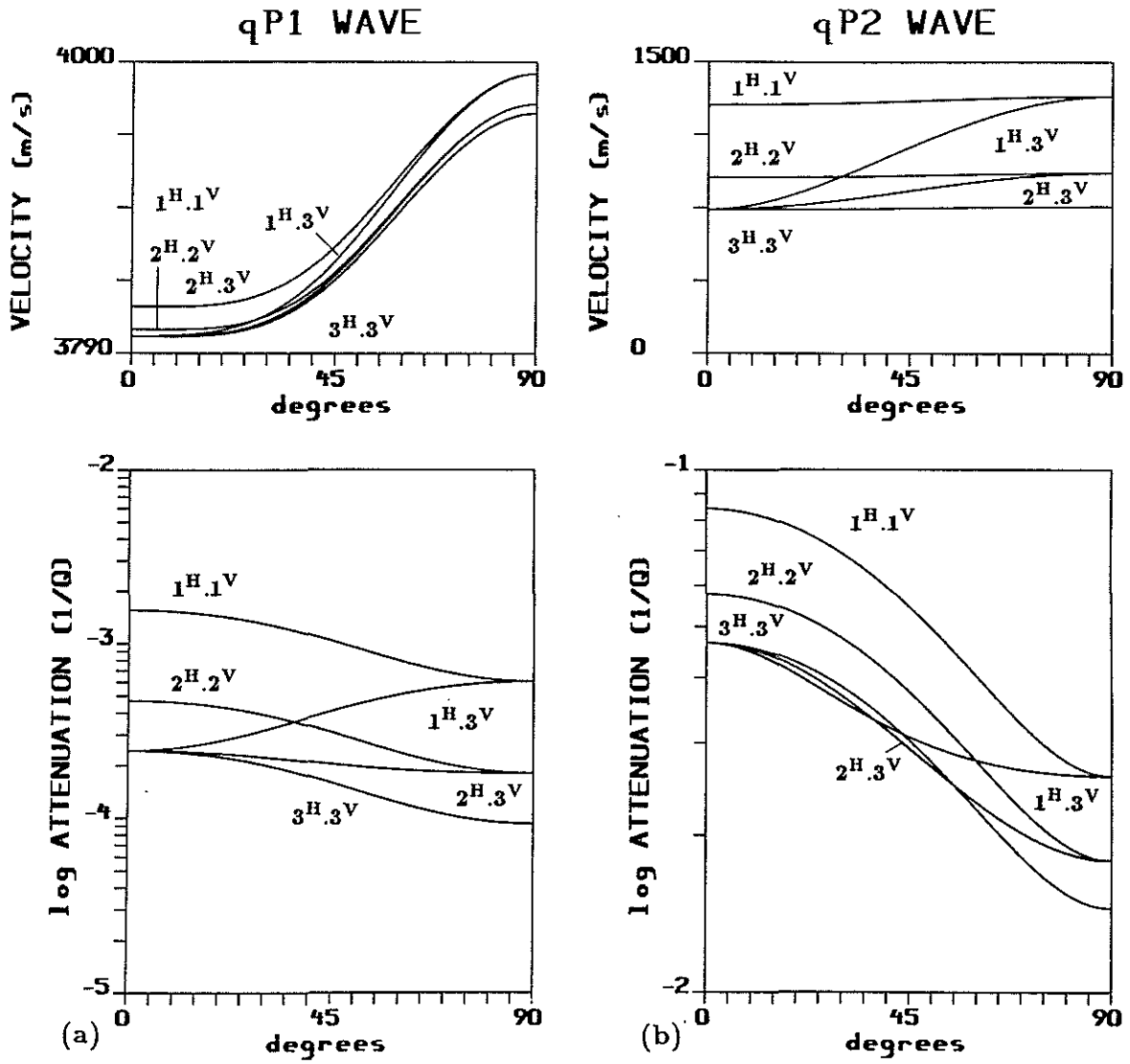

Figure 9: Anisotropic mass coupling coefficient (tortuosity) effects as a function of the angle of propagation with respect to the vertical at a frequency equal to 10^7 Hz. The superscripts H and V denote the horizontal plane and the vertical direction. The affected numbers refer to the tortuosity value. The formation is the transversely isotropic sandstone.

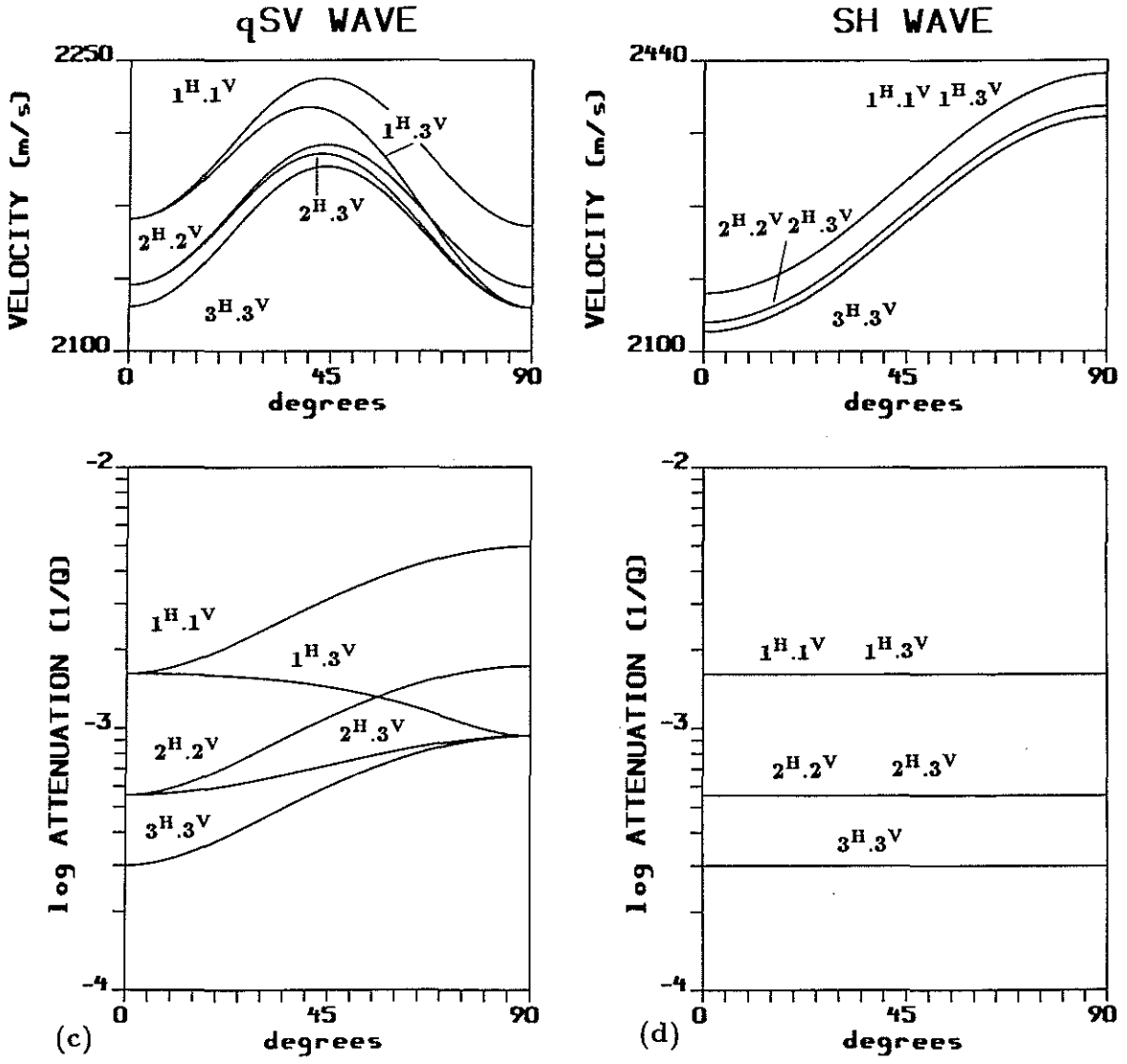
qSV WAVE
SH WAVE
VELOCITY (m/s)
2250
2100
2440
0
45
90
degrees
$1^H.1^V$
$1^H.3^V$
$2^H.2^V$
$2^H.3^V$
$3^H.3^V$
log ATTENUATION (1/Q)
-2
-3
-4
(c)
(d)